Physicochem. Probl. Miner. Process., 58(4), 2022, 151600

http://www.journalssystem.com/ppmp

Physicochemical Problems of Mineral Processing

ISSN 1643-1049

Modelling the power draw of tumbling mills: A comprehensive review

Mohammad Hasan Golpayegani, Bahram Rezai

Mining engineering faculty, Amirkabir University of Technology, Tehran, Iran

Corresponding author: Rezai@aut.ac.ir (Bahram Rezai)

Abstract: Optimizing power consumption in grinding, the most consumed stage in the mining industry, plays an influential role in reducing operating costs. Obtaining an efficient model to predict tumbling mills' power consumption accurately took the attention of researchers, mineral processing engineers, and tumbling mill manufacturers. This article comprehensively reviews the published mill power models and the most critical studies on this topic since 1919. Furthermore, the employed approaches for modelling the tumbling mills' power draw, the incorporated parameters into the developed models, the models' performances in predicting the industrial mills' power draw, and the potential gaps in the available literature are discussed. Moreover, based on the shortages identified in this review, some recommendations have been made to enhance the modelling mill power draw.

Keywords: *g*rinding, tumbling mills, power draw, modeling approaches

1. Introduction

Millions of tons of different metals are produced annually worldwide, and tumbling mills are the heart of this production process. It is reported that grinding accounts for approximately 40% of the total mining energy consumption and more than 50 % of mineral processing plants' operating costs (U.S. DOE 2007). Besides, falling the average grade of ores in most mines worldwide causes dramatic increases in the cost of energy per unit of produced metal (Valery and Jankovic, 2002). Thus, optimizing and reducing power consumption are considered essential factors in milling operations' design to decrease grinding and related operations costs. To this end, a method capable of predicting the mills' power draw can be a practical and vital tool for researchers, designers, and plant managers (King, 2001). According to the existing theories, the description of the charge shape inside the tumbling mills and milling operation analyzing approach comprised of energy balance, torque-arm, friction force, and discrete element method are regarded as two vital parameters in modelling the power draw. Besides, the milling operation is an interactive system, as illustrated in Fig. 1. From Fig. 1, it is evident that milling operation is interrelated to mill operating parameters, ore characteristics, and mechanical components. Therefore, any change in these parameters affects the mill power draw. Accordingly, various parameters can play a role in how a capable model can predict power draw in a given operating condition. Although numerous models have been published to predict the mills' power draw, no equation incorporates all effective parameters. Therefore, power draw models have been gradually evolved to achieve the highest correlation with industrial data. This paper introduces developed models to predict the power draw of tumbling mills, explains the employed approaches in preparing them, and assesses their performances. Moreover, the affecting parameters incorporated into developed models are discussed to identify shortcomings and provide recommendations for future studies.

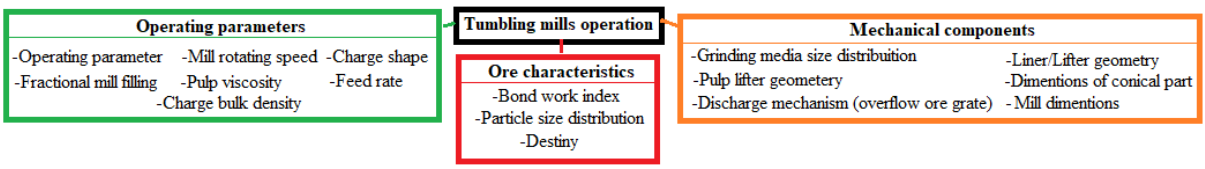

Fig. 1. Grinding as an interactive system

DOI: 10.37190/ppmp/151600

2. Modelling approaches

Various approaches have been utilized to develop models for power draw prediction of tumbling mills. Accordingly, developed models can be classified under two general categories: empirical and fundamental. Moreover, the fundamental models can be classified under four subsets: energy balance, torque-arm, friction approach, and discrete element method (DEM). Fig. 2 shows the classification of different approaches to modelling the tumbling mills' power draw (Morrell, 1993). It must be noted that recently the smoothed particle hydrodynamics (SPH) and computational fluid dynamics (CFD) have contributed to the DEM and understanding of the vague issues regarding the mill charge dynamic process. However, the mentioned classification is still valid because the SPH and CFD have been used as auxiliary tools for the DEM.

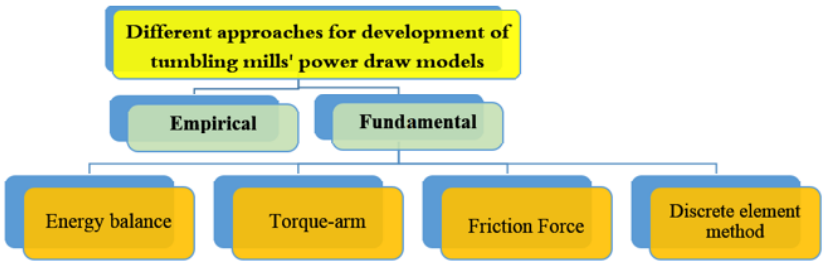

Fig. 2. The general *classification* of developed models for power draw prediction of tumbling mills.

2.1. Empirical models

Despite recent advances in the fundamental models, some energy-consuming phenomena have not been incorporated because of the lack of complete understanding. These phenomena include heat generation due to friction, attrition and abrasion breakage of the rock charge, rotational motion of the grinding media during raising from toe to shoulder, and gearbox and bearings' friction (Morrell, 1993; Daniel et al., 2010). As a result, mill manufacturers and engineers often use empirical models for grinding circuit design. This section describes the empirical equations and then assesses their predictive capability.

2.1.1. Models' description

Several empirical models have been developed for predicting the tumbling mills' power draw. Using the dimensional analysis method, Rose and Evans (1956) investigated the effect of a wide range of operating and design parameters and published the following equation:

$$P = 3.13D^4LN^3N_c^{-2}\rho_b\left(1+0.4\frac{\rho_p}{\rho_b}\right)\left(3.35J_t+1.3372J_t^2-9.1602J_t^3\right) \quad (1)$$

where P is the power draw (kW), D and L are the ball mill internal diameter and length (m), respectively, ρ_b is the balls' density (tonnes/m^3), ρ_p is the slurry density (tonnes/m^3), N is the rotational speed (revs/sec), N_c is the mill critical speed (revs/sec), and J_t is the fractional mill filling.

Bond (1961) established a simple equation to predict the ball mills' power draw by considering the effect of the mill dimensions, rotating speed, fractional mill filling, and balls' bulk density. Besides, he implicitly modelled the impact of make-up balls diameter and discharge level on grate discharge mills' power. Bond published Equation 2 for overflow discharge ball mills. Furthermore, to calculate grate discharge mills' power, he proposed the multiplying factor of 1.15.

$$KW_b = 4.893D^{0.3}\left(3.2-3V_p\right)C_s\left(1-\frac{0.1}{2^{(9-10C_s)}}\right)-1.102\left(\frac{B-12.5D}{50.8}\right) \quad (2)$$

where KW_b is the power consumption per balls' tonne (kW/ton), D is the mill diameter (m), C_s is the fraction of critical speed, V_p is the fractional mill filling and B is the make-up balls' diameter (mm). Part $\left(1-\frac{0.1}{2^{(9-10C_s)}}\right)$ is the Bond's speed function indicating the relationship between power and rotating speed. For determining the total power draw, the KW_b value must be multiplied by the balls' total mass (W) as follow:

$$W = J\pi\frac{D^2}{4}L(1-\varphi)*\rho_b \quad (3)$$

where J is the mill filling, D and L are the mill's diameter and length (m), ρ_b is the balls' density (tonnes/m^3), and φ is the grinding media voidage.

Moys (1993) stated that Bond's equation should be improved to predict accurately the power draw of ball mills running at high rotating speed. Based on observing balls' behaviour in a laboratory ball mill running at high rotating speeds, he classified the mill charge into two parts: a non-centrifuging portion that draws power and a centrifuging layer that draws no power. He found that the charge's tendency to centrifuge increases at high mill speeds, high lifter profiles, and high slurry viscosity, leading to increased centrifuging layer thickness and subsequently decreased the power draw. Accordingly, the following power equation was developed:

$$P = KD_{eff}^{2.3}\text{Sin}\alpha\ \rho_L\left(\left(\frac{J-4\delta_C(1-\delta_C)}{(1-2\delta_C)^2}\right)-\beta\left(\frac{J-4\delta_C(1-\delta_C)}{(1-2\delta_C)^2}\right)^2\right)N_{eff} \quad (4)$$

where P is the power draw (kW), D_{eff} is the mill effective diameter (m), α is the charge's angle of repose (radians), ρ_L is the bulk density of the charge (kg/m^3), J is the fractional mill filling, β is a parameter, N_{eff} is the fractional speed at $D=D_{eff}$, K is a constant, and δ_C is the centrifuging layer's thickness (m) which is obtained through following equation:

$$\delta_C = J^{\Delta J e^{\frac{-(N^*-N)}{\Delta N}}} \quad (5)$$

where J is total fractional filling, N is the mill rotating speed (rpm), and ΔJ, N^*, and Δ_N are functions of liner profile design and slurry viscosity.

Morrell (1993) developed two significant models, including fundamental (C-model) and empirical (E-model). He provided an empirical model by applying an industrial database and considering the mill diameter, mill length, mill rotating speed, bulk density of the mill charge, and the fractional mill filling as parameters affecting the power draw (Eq. 6). Besides, the effect of the mill shell's conical-end sections, the discharge mechanism, and energy losses relating to mechanical and electrical components have been encompassed in the Morrell E-model. Morrell divided the gross power into two parts: "no-load power," indicating the required power to overcome losses in the mills' motor, gearbox, and bearing (part 1 of Equation 6), and "net power," demonstrating the power transmitted to the mill charge (part 2 of Equation 6). The Morrel E-model for determining the gross power draw is as follows:

$$P_G = \left\{11\times\left(r_m^{2.5}LC_s\right)^{0.861}\right\}+\left\{k^*\left(D^{2.5}L\rho_c J_t\frac{\left((5.9726C_s-4.4258C_s^2-0.98524)-J_t\right)}{\left((5.9726C_s-4.4258C_s^2-0.98524)\right)^2}\right)\times\left[C_s\left(1-\left(0.046+0.135J_t\right)e^{-A\left(0.954-0.135J_t-C_s\right)}\right)\right]\right\} \quad (6)$$

where P_G is the gross power (kW), L is the mill effective length (m), r_m is the mill effective radius (m), C_s is the fraction of critical speed, D is the mill effective diameter (m), ρ_c is the bulk density of charge (tonnes/m^3), A is a parameter and J_t is the total fractional mill filling. Moreover, the " k " parameter is the calibration factor for considering heat losses resulting from friction inside a mill (between balls or between balls and liners), breakage by abrasion mechanism, and rotating the grinding media.

Van Nierop et al. (2001) attempted to enhance Moys' model's accuracy (Eq. 4) through a meticulous investigation of load behavior inside an industrial ball mill. To this end, they utilized different instruments, including conductivity probes to measure the load behavior aspect, a load cell to measure the load mass, and a power meter to determine the power draw. Accordingly, they concluded that the power draw decreases by overloading the mill due to forming a centrifuging layer whose thickness enhances by increasing the load mass. Besides, they found that the centrifuging layer's thickness is varied along the mill length and can be divided into three sections: the feed, the middle, and the discharge sections. The following equation gives each section centrifuging layer's thickness:

$$\delta'_{c,i} = \delta_c + \lambda d_{c,i} \quad (7)$$

where δ_c is the centrifuging layer's thickness from Moys' model (m), $\delta'_{c,i}$ is the adjusted thickness (m), λ is a function indicating the degree of centrifuging at probe i, $d_{c,i}$ is the maximum thickness of the centrifuging layer at probe i, and "i" is the embedded conductivity probe at each mill's section.

Tsakalakis and Stamboltzis (2004), using a database from Denver ball mills and applying multiple linear regression method, established the following simple equation for predicting the ball mills' power draw:

$$P = 10.38f_cD^{2.5}L\rho f_L(1-f_L) \quad (8)$$

where P is the power draw (kW), D is the mill effective diameter (m), L is the mill effective length (m), ρ is the balls' bulk density (tonnes/m^3), f_L is the the total fractional filling, and f_c is the fractional speed. According to the literature, the feed ore competence, including lithology, hardness and particle size distribution, is a remarkable parameter affecting tumbling mills' energy consumption (Bond, 1961; Morrell, 2009). The effect of feed size distribution has been reported more than the ore characteristics, especially in the SAG mills (Razani et al., 2018). Since the different feeds with different particle size distributions can have the same F_{80} (the 80% passing feed particle size), Silva and Casali (2015) stated that the F_{80} could not represent the size distribution appropriately. Consequently, by considering the fraction of -6+1 inch as the independent variable affecting SAG mills' power draw and utilizing the four industrial SAG mills' operating data, they developed the following power draw equation:

$$P = D^{2.5}L\left\{0.0348\left(\%\text{-}6''+1''\right)+26.4J_b\text{-}6.7\frac{N}{N_c}+\frac{4}{S}\right\} \quad (9)$$

where P is the SAG mill's power draw (kW), D and L are the mill internal diameter and length (m), respectively, J_b is the fractional mill filling by steel balls, $\frac{N}{N_c}$ is the fraction of SAG mill critical speed, and S is the percent solids of the slurry.

2.1.2. Assessing the empirical models' performances

This section discusses the empirical models' performance, advantages, and disadvantages according to the available information. Morrell's thesis and subsequent papers discuss mill power models' performances, as discussed in more detail in this review. Of course, Morrell's studies have not covered some models including, Van Nierop et al., Tsakalakis and Stamboltzis, and Silva and Casali. In this work, we have tried to examine the reasons for the accuracy or inaccuracy of the mill power models more carefully and critically with aimed at providing solutions for the progress of models.

Fig. 3 shows the performances of Rose and Evans' model, Bond's model, and the Morrell E-model, Tsakalakis and Stamboltzis's model, and Silva and Casali's model in predicting the industrial tumbling mills' power draw. As shown in Fig. 3a and 3b, there is an apparent disagreement between predicted data by the Rose and Evans' model and actual ones for both ball and AG/SAG mills. Although Rose and Evans' model was developed for the ball mills, it tends to under-predict the power draw which could be due to the small scale of the ball mills used in this study (less than 3 inches), which has led to a defective implementation of actual conditions in the laboratory. Consequently, the effect of lifter specifications, balls' size, as well as the slurry properties on the ball mills' power have reported negligible in Rose and Evans' investigation. Furthermore, ignoring the motor and gearbox energy is another reason for the under-predicting of this model.

The diagram of Fig. 3c demonstrates the suitable capability of Bond's model in predicting the ball mills' power draw; this is why engineers use Bond's model for plants' design. In contrast, the associated Fig. is inappropriate for AG/SAG mills which is comprehensible because Bond's model was not developed for AG/SAG mills. One of the remarkable shortcomings of Bond's model and all developed models is the considered value for grinding media's voidage (parameter of "φ" in Equation 3). The "φ" value is assumed to be 0.4 in all developed models, while documented studies on this parameter's determination are unavailable. On the other hand, based on published studies regarding the particles bed's voidage, the value of 0.4 is reported for a bed of the mono-sized spherical particles after exerting vibration to the bed (Yang, 2003). Since the grinding media includes multi-sized particles, its voidage can differ from 0.4. Hence, ignoring the precise voidage value is a fundamental shortcoming in all developed models. We believe that it is possible to make a relationship between balls' size distribution (by scaling down the actual size of balls) and balls' voidage through an empirical study which can be considered for future research. The prominent Bond's model disadvantage is the non-incorporation of rock charge and slurry specification. Determining the grinding media's voidage as mentioned and replacing the balls' bulk density with the bulk density of the mixture of grinding media and slurry in Equation 3 may improve the performance of Bond's model, which needs to be investigated.

As shown in Figs. 3e and 3f, the Morrell E-model has good predictive capability in all cases. Of course, the standard deviation of the Morrell E-model's relative error is reported slightly higher than Bond's model in the ball mill data. The Morrell E-model's most crucial advantage in increasing its prediction accuracy is considering the motor and gearbox energy losses reported 4% and 3% for the

motor and gearbox, respectively (Morrell 1993). Generally, the resistance temperature detectors (RTDs) equipped with transmitters are installed on the mills' motor and gearbox to protect this equipment in abnormal operating conditions, using process control logic (Nietro and Ahrens 2007). We believe that researchers can use the data collected from these instruments in the plants' supervisory control and data acquisition system (SCADA) to improve the power models from the heat loss point of view. Moreover, the technical data of heat losses in the main electrical and mechanical components are available from mills' manufacturers, which researchers can use to prepare an empirical heat loss model.

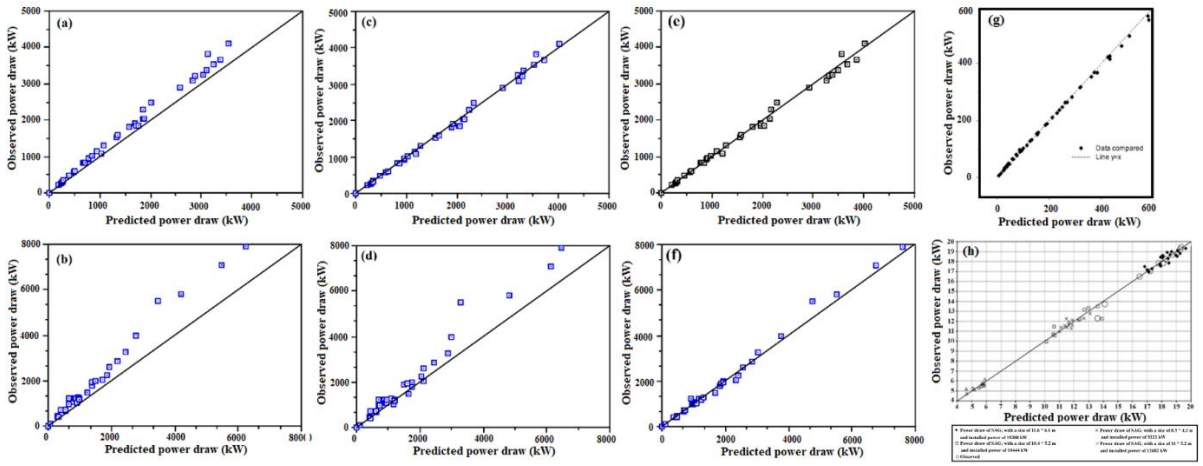

Fig. 3. Performance of power draw models. (a) Ball mills' predicted power by Rose and Evans' equation, (b) AG/SAG mills' predicted power by Rose and Evans' equation, (c) Ball mills' predicted power by Bond's model, (d) AG/SAG mills' predicted power by Bond's model, (e) Ball mills' predicted power by the Morrell E-model, (f) AG/SAG mills' predicted power by the Morrell E-model (Morrell, 1993). (g) The predicted power by Tsakalakis and Stamboltzis's equation versus the Denver ball mills' data (Tsakalakis and Stamboltzis, 2004). (h) Observed and predicted power draw of four different industrial SAG mills by Silva and Casali's equation (Silva and Casali, 2015)

According to Eq. 4, the most crucial drawback of Moys' model and its modified version (by Van Nierop et al.) is the existence of parameters (β, ΔJ, N^* and Δ_N) that must be determined based on laboratory studies, making it difficult to validate with industrial data. Hence, the only evaluation of these models' performance was conducted by Van Nierop et al. (2001). They found that the revised model can accurately estimate the power draw of a 4.3 diameter mill running at a high fraction of critical speed. However, its dependence on conductivity probe data makes it challenging to use in the industry. Although Moys' model has some limitations, its attempt to consider the effect of lifter design on mill power is its strength. No model can do this except for DEM.

Fig. 3g shows good agreements between the predicted power by Tsakalakis and Stamboltzis' equation versus the Denver ball mills' data. Although this equation aligns with Denver mills' data, no documentary report relating to applying it in the industrial mills. Like Bond's model, non-considering the ore and slurry characteristics is the most critical disadvantage of this model.

Fig. 3h demonstrates that the performance of Silva and Casali's model for predicting the power draw of the SAG mills' with the medium and high-power is good. This model's most crucial advantage is that process engineers can use it to optimize the grinding circuit's power consumption by adjusting the feed particle size distribution. It can be implemented by optimizing the blasting pattern, changing the primary crusher's closed side setting, or employing the segregation phenomenon in the stockpile. For instance, the SAG mill feed rate can be increased by increasing the fractional mill filling of balls as grinding media and decreasing the intermediate size fraction (-6 "+1") without affecting the grinding circuit's power consumption. Given that the impact mechanism is dominant in SAG mills and the amount of power consumption is associated with ore's Bond work index, We believe that the intermediate size fraction (-6 "+1" in the original model) may vary for different minerals and SAG mills' dimensions. Hence, investigating it can lead to an increase in Silva and Casali's model's accuracy. Overall, the most significant advantage of empirical models is that they are supported by industrial and

laboratory databases. Thus, they can provide a plausible prediction of the power draw in tumbling mills' normal operating conditions. For this reason, Bond's model and Morrell's E-model have been used in the industry (Daniel et al., 2010). The common empirical models' disadvantage is that they are developed based on a particular range of operating conditions; therefore, they cannot accurately predict the power draw beyond a specific range of operational parameters. Besides, since the empirical models are not based on analysis of physical laws and statistical regression techniques are used to develop such models, these equations do not provide insight into tumbling mills' physical behaviour.

2.2. Fundamental models

A phenomenological relationship has been provided in the fundamental models between the power draw and affecting parameters through basic physics laws. Since the DEM is developed based on computer computing power progression, we have provided it separately from the other three approaches in one section.

2.2.1. Developed models based on Energy balance, Torque-arm, and Friction Force approaches

Most mathematical power models have been derived from the energy balance and torque-arm basic equations. In the energy balance approach, the calculation of potential and kinetic energy is used to model the mills' power draw based on the following basic equation (Morrell, 1993; Walker et al., 2001):

$$P = \frac{E}{t} \tag{10}$$

where P is the mechanical power (Nm/s), E is the kinetic or potential energy (Nm), and t is the time (s). The most straightforward equation, used to model the mills' power, is the torque-arm equation, which is defined as follows (Walker et al., 2001; Morrell 2019):

$$P = 2\pi\tau N \tag{11}$$

By supposing the mill charge as a locked mass (see Fig. 4a) and considering that weight is equal to mass × gravitational acceleration, the required power to rotate a mill is given by (Morrell, 2019):

$$P = 2\pi WOG \sin\alpha\, N \tag{12}$$

where W is the charge weight (N), part OG sin α is the lever arm distance (m), and N is the rotating speed (revs/sec). Various models have been developed based on Equation 12 (Harris et al., 1985; Liddell and Moys, 1988; Fuerstenau et al., 1990; Morrell, 1993).

The friction force approach assumes that transferring energy from the mill to the charge is conducted by the friction forces between the mill shell and the moving charge. By supposing the constant value for the particle's tangential velocity (V_r) along a streamline at a radial distance (r), the tangential component of a supposed element's weight shown in Fig. 4b must be equal to a friction force in the opposite direction (Morrell, 1993). Since power is the result of force and velocity, the following general equation can estimate the power draw (Walker et al., 2001):

$$P = FV \tag{13}$$

where P is the power (Nm/s), F is the friction force (N), and V is the particle's tangential velocity (m/s). Considering the mill charge as a mass limited between toe angle (θ_T), shoulder angle (θ_S), mill inner radius (r_m) and charge inner surface(r_i), as shown in Fig. 4b, the net required power for moving the charge is given through friction force approach as follow (Morrell, 1993):

$$P = 2\pi g L \rho_c \int_{r_i}^{r_m} \int_{\theta_T}^{\theta_s} V_r\, r \cos\theta\, d\theta\, dr \tag{14}$$

where P is the power draw (kW), g is the gravitational acceleration (m/s^2), and V_r is the particle's tangential velocity (m/s). Morrell is the only researcher who has used this approach (Morrell, 1993).

2.2.1.1. Models' description

A description of charge motion must first be provided to develop a fundamental power equation (Van Nierop et al., 2001). Davis (1919) was the first person that establishes a relationship between charge motion and power draw using the energy balance approach. In his description, the particles move in a

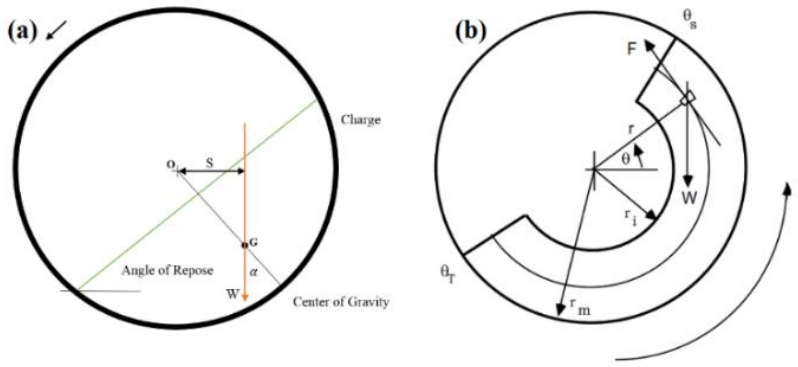

Fig. 4. Schematics for the friction force and torque-arm approaches. (a) Charge shape used by the torque-arm approach (Morrell, 2019). (b) Charge shape used by the friction force approach (Morrell, 1993)

locked manner in a circular path until a point where the gravitational and centrifugal forces balance. At this point, particles experience a parabolic free fall until they impact the bed, and afterward, they return to the circular path again (see Fig. 5a). Consequently, Davis developed the following equation:

$$P = Wr^{1.5}\left(0.0045\frac{\left(1-K^3\right)}{\left(1+K^2\right)^{0.125}} - 0.0037\frac{\left(1-K^5\right)}{\left(1+K^2\right)} + 0.00088\frac{\left(1+K^7\right)}{\left(1+K^2\right)^{0.625}}\right) \tag{15}$$

where P is the power draw (hp), r is the mill radius (ft.), W is the charge mass (pounds), and K is a function of mill volume occupied by a part of the charge that has no free flight.

Hog and Fuerstenau (1972) remarked that Davis' description has two shortcomings: (1) the quantity of material (ball filling) has been ignored, and (2) the circular paths shown cannot cross each other, which it is an unrealistic assumption. Hence, they provided a new description in which the mill charge includes two parts: a 'static' part moved with the mill shell and a 'shear' region in which particles flow down on the charge's surface (see Fig. 5b). In this description, the mill motor supplies energy to raise balls in circular paths through the static part from the toe to the shoulder. Since the milling system is in the dynamic equilibrium condition, an assumed particle should have the same energy at the same location. Hence, the particles' potential energy ($mg\lambda_t$) in the bed's static part is completely lost in the shear zone. Based on this, the following equation was derived using the energy balance approach:

$$P = \frac{2}{3}\rho_{bulk} g^{\frac{3}{2}} L N_c \left(\frac{D}{2}\right)^{2.5} \sin^3\theta_0 \sin\alpha \tag{16}$$

where P is the power draw (kW), D is the mill effective diameter (ft.), L is the mill effective length (ft.), ρ_{bulk} is the mill charge's bulk density (tonnes/m^3), α is the charge's angle of repose (typically in the range of 30° to 35°), N_c is the fractional speed, and θ_0 is the filling angle (in radians).

Harris et al. (1985), by employing a database from mill manufacturers and using Hog and Fuerstenau's description of charge motion, improved the Hog and Fuerstenau's equation and developed the following general equation using the torque-arm approach:

$$P = KD^n L\rho_{bulk}\gamma N_c J(1-aJ) \tag{17}$$

where P is the power draw (kW), D is the mill diameter (m), L is the mill length (m), ρ_{bulk} is the mill charge's bulk density (tonnes/m^3), N_c is the fractional speed, J is the fractional mill filling, and K, γ and a are parameters. Many models (Bond, 1961; Hogg and Fuerstenau, 1972; Liddell and Moys, 1988 and Austin, 1990) can be derived by applying Equation 17.

To improve Harris et al.'s model, Liddell and Moys (1988) conducted an experimental study using a glass-fronted laboratory mill and a high-speed camera on the mill charge behavior and divided the mill charge into four parts (see Fig. 5c). Based on this, they implicitly incorporated slurry rheology on the power draw by defining a speed function for the first time. They concluded that the power draw increases with a simultaneous increase in the slurry viscosity and rotating speed. Finally, using the torque-arm approach, the following power equation was developed:

$$P = 9.69D^{2.5} L\rho_{bulk}\delta N_c J(1-1.06J) \tag{18}$$

where P is the power draw (kW), D and L are the mill effective diameter and length (m), respectively, ρ_{bulk} is the mill charge's bulk density (tonnes/m^3), δ is the speed function, N_c is the fractional speed, and J is the fractional mill filling.

The first explicit incorporation of slurry viscosity into the power equation has been accomplished by Fuerstenau et al. (1990). Accordingly, they provided a new description of charge motion supposed that the charge encompasses two different parts: a 'cataracting/centrifuging fraction,' which is affected by the slurry viscosity, and a 'cascading fraction' that is not influenced (see Fig. 5d). Subsequently, they divided the required mill power into P_{cs} and P_{ct} associated with cascading and cataracting/centrifuging fractions, respectively. Moreover, they considered the energy losses by frictional components (P_f) and derived the following equation by using the torque-arm approach:

$$P = P_{cs}+P_{ct}+P_f=\left[\frac{2NW_1g(D-d)}{3J_1}\emptyset(J_1)\sin\alpha\right]+[2\pi NW_2g\,s\cos\gamma]+\left[Cexp^{(-Kt)}\right] \quad (19)$$

where P is the power draw (kW), N is the rotational rate (revs/sec), W_1 and W_2 are the weight of cascading and cataracting/centrifuging fractions (N), respectively, D is the mill diameter (m), d is the ball diameter (m), J_1 is the fractional filling by cascading fraction, $\emptyset(J_1)$ is the function of fractional filling by cascading fraction, α is the mill charge's angle of repose, s is the lever-arm length (m), γ is an angle (in radians) which determines the tangential component of the W_2 , t is the grinding time (s), and K and C are constants that should be obtained from experiments.

Austin (1990) attempted to develop a particular equation for predicting the SAG mills' power draw using the energy balance approach and Hog and Fuerstenau's idealized description of charge motion. However, he expressed that Hog and Fuerstenau's model neglected the material's kinetic energy. Hence, he incorporated the supplied kinetic energy by the mill to move material into Hog and Fuerstenau's model and developed the following equation by employing the energy balance approach:

$$P = 10.6D^{2.5}L(1-1.03J)\rho_c\left(\left(1-\frac{0.1}{2^{9-10C_s}}\right)\right) \quad (20)$$

where P is the power draw (kW), D and L are the effective diameter and length of mill (m), C_s is the fractional speed, J is the fractional mill filling, and ρ_c is the charge bulk density (tonnes/m^3).

Morrell (1993) claimed that the power equations had been developed based on unrealistic descriptions of charge motion. Hence, using the photographic technique, he provided a graphic source of the charge shape in the various operating conditions comprising the fractional mill filling, rotating speed, and lifter shape. He found that the power draw results from a part of the charge with a crescent shape named active charge that exerts a force on the tumbling mills' shell. Fig. 5e illustrates the shape of the active charge inside a grate discharge mill in which the mill charge fills the grinding media's voidage. While in the overflow discharge mills, the surplus slurry forms a slurry pool besides grinding media (see Fig. 5f), causing a reduction in the power draw due to assisting in rotation by slurry in the toe region (Morrell, 2016). Thus, Morrell's description of the charge motion can justify the power draw differences between the grate and overflow discharge mills. Morrell applied all three approaches comprising torque, energy balance, and friction force and concluded that the equation derived from the energy balance approach is more comprehensive. Accordingly, the Morrell C-model was presented as follows:

$$P_{Gross}=11\times\left(r_m{}^{2.5}LC_s\right)^{0.861}+\frac{\pi gLN_mr_m}{3(r_m-Zr_i)}\left\{2r_m^3-3Zr_m^2r_i+r_i^3(3Z-2)\right\}\left\{\rho_c(\sin\theta_S-\sin\theta_T)+\rho_P(\sin\theta_T-\sin\theta_{TO})\right\}+L\rho_c\left\{\frac{N_mr_m\pi}{3(r_m-Zr_i)}\right\}^3\left\{(r_m-Zr_i)^4-r_i{}^4(Z-1)^4\right\} \quad (21)$$

where P_{Gross} is the gross power (kW), r_m and L are the mill effective radius and length, respectively (m), C_s is the fractional speed, ρ_c is total charge's density (tonnes/m^3), ρ_P is the slurry density (tonnes/m^3), N_m is mill rotational rate (revs/sec), r_i is the radial distance of the charge's inner surface from the rotating axis (m), θ_T is the toe angle (radians), θ_S is the shoulder angle (radians), Z is a function of fractional mill filling and θ_{TO} is the slurry toe angle (see Fig. 5f).

In the grate discharge mills, the parameters, including the grates' open area, the mill aspect ratio, feed flow rate, mill rotating speed, and the performance of pulp lifters affect the grate's performance, the mill's flow capacity and consequently the power draw (Powell and Valery, 2006; Morrell, 2016). For instance, by increasing the feed flow rate, the slurry hold-up occurs so that the slurry fills the grinding media voidage progressively, and a slurry pool is formed that declines the power draw (Morrell, 2016).

To consider the slurry pool's effect on the power draw, Latchireddi (2002) incorporated it into the Morrell C-model by estimating the fractional slurry hold-up leading to the designation of the slurry toe position (θ_{TO}) and more accurate prediction of power draw:

$$J_S=\eta\ \gamma^{n_1} A^{n_2}\ J_t^{n_3}\ C_s^{n_4}\ Q^{n_5}\ D^{n_6} \tag{22}$$

where J_S is the net fractional slurry hold-up, A is the fractional open area of the grate, J_t is the fractional volume of grinding media, C_s is the fractional speed, Q is the slurry discharge flow rate (m^3/hr), D is the mill diameter (m), η is a function of slurry viscosity, γ is the mean relative radial position of the grate hole (m) and n_1 to n_6 are functions of pulp lifter.

The net power draw is affected significantly by the charge density, which is directly proportional to the ore's specific gravity. The developed models have not considered the ore's hard components' building-up effect on the charge density inside the mills. This phenomenon is related to different parameters: feed blending, breakage function variability, breakage rate, retention time, and various minerals' specific gravity in the ore composition. Bueno et al. (2013) attempted to upgrade the Morrell C-model by considering ore's hard components building-up. To this end, they used the AG/SAG JKSimmet simulation package, which applies the Morrell C-model. Using this simulation package and analyzing the behaviour of both hard and soft components of ore by using the separate perfect mixing model, they made a balance between ore components and their relative specific gravities. Based on this, They boosted the JKSimmet package's ability by developing an AG/SAG multi-component. They concluded that the multi-component model has an excellent ability to describe ore's hard components building-up, leading to a decrease in charge density and SAG mills' power draw.

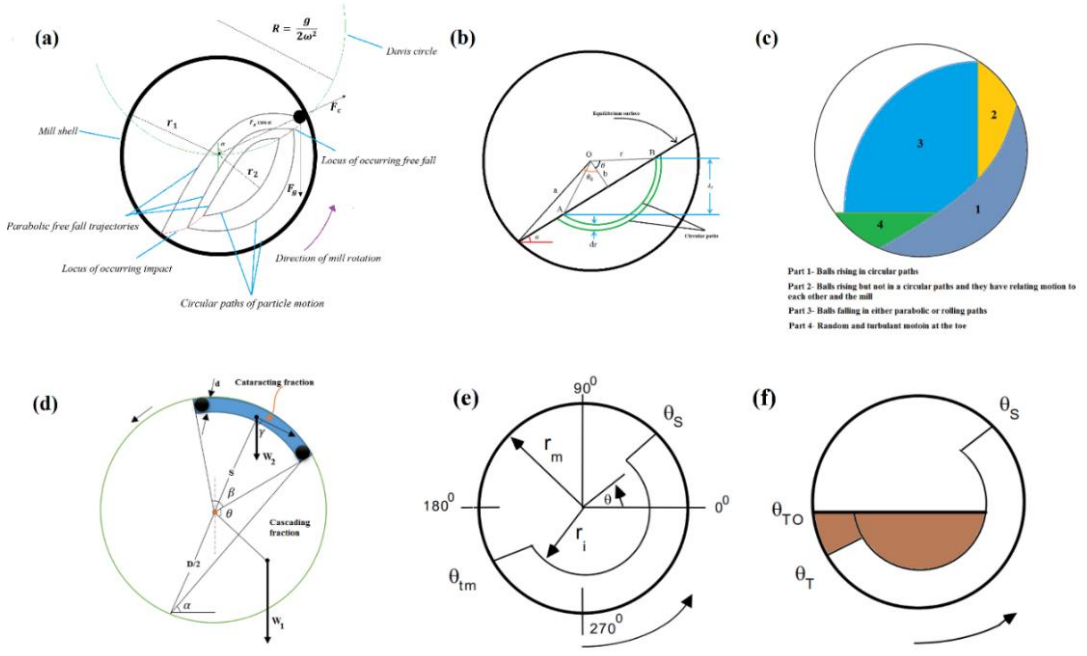

Fig. 5. Schematic of descriptions of charge motion. (a) Davis' description (Davis, 1919), (b) Hog and Fuerstenau's description (Hogg and Fuerstenau, 1972), (c) Liddell and Moys' description (Liddell and Moys, 1988), (d) Fuerstenau et al.'s description (Fuerstenau et al., 1990), (e) Morrell's description for Grate discharge mills, (f) Morrell's description for overflow discharge mills

2.2.1.2. Assessing the fundamental equations' performance

Morrell's thesis and subsequent papers discuss some mill power models' performances. The main point is that the original and modified Morrell C-model versions have not been reviewed accurately yet, which is considered in this work. Moreover, we believe that Hogg and Fuerstenau's model as an acceptable model in the industry needs progress and improvement. Hence, this section emphasizes the assessment of Hogg and Fuerstenau's model and the Morrell C-model and related developments.

Literature indicates that Austin's model tends to sharply over-predict for ball mills, which is understandable because it was not developed for ball mills (Morrell, 1993). Besides, the presented data regarding SAG mills in the literature shows an over prediction of Austin's model. Likewise, it is reported that Harris et al.'s model tends to over-predict for both ball mills and AG/SAG mills. These shortcomings can be related to the unrealistic ideal load shape used in developing these models.

Figs. 6a and 6b indicate the performance of the Morrell C-model (Morrell, 1993). From these Figs., it is evident that the Morrell C-model's prediction results are marginally closest to actual data for both ball and AG/SAG mills. Similarly, other evaluation studies indicate that the Morrell C-model's prediction results have good agreement with wet and dry industrial ball mills data (Erdem et al., 2004; Basirifar et al., 2018). Doll (2016) assessed the predictive capability of Austin's model and the Morrell C-model using a database including 49 AG/SAG mills from all over the world. He reported that both the mean and standard deviation of the Morrell C-model are considerably lower than Austin's model. The Morrell C-model's most notable advantage is the new description of the charge's behaviour in which the power draw associated with the slurry is considered separately from the grinding media. Furthermore, another advantage is that this model includes the energy loss in the mechanical and electrical components to estimate the motor's input power. It should be noted that the attempts made by Latchireddi (2002) in incorporating the slurry pool's effect, and Bueno et al. (2013) in considering ore's hard components building-up, has led to an increase in the Morrell –C-model's accuracy. Fig. 6c illustrates the actual and predicted power draw (estimated by the Morrell C-model) of SAG mills with slurry pools in which it is the assumption that there is no slurry pull. As can be seen, by assuming standard operating conditions without considering the slurry pool, the predicted power draw is considerably higher than the measured values. In contrast, by considering the slurry pool's effect, an acceptable and tangible agreement between the actual and modified predicted power draw of SAG mills can be observed, as shown in Fig. 6d (Morrell, 2016).

Although the Morrell C-model can be considered a more comprehensive and accurate equation compared to others, its development has some drawbacks. For instance, the voidage of the active charge, which has a remarkable effect on the power, has been assumed to be equal to the static voidage of balls (0.4). While, the active charge is dynamic, and its voidage can change with changing operating conditions such as rotating speed, fractional mill filling, and balls' size distribution. On the other hand, the static voidage itself also needs further investigation. Hence, we propose investigating the possibility of developing a comprehensive equation for determining the dynamic voidage that can increase the accuracy of the Morrell C-model. As mentioned, this issue can be examined through an empirical study by using scaled-down balls. Additionally, based on some consistent work (Soleimani et al., 2015; Soleimani et al., 2016), another shortcoming is that Morrell C-model may not precisely capture the effect of mill speed on the power draw. These works clearly show that power draw increase with the mill speeds faster than predicted by Morrell C-model. We believe that using the results of these studies and conducting future investigations, especially on industrial mills, the Morrell C-model can be modified by defining a speed correction factor. The shortcoming of the Morrell C-model related to the speed effect can be associated with the crescent-shaped load behavior. Indeed, Morrell assumed the crescent-shaped load has a locked state, which is unrealistic and has implications. This issue needs to be further investigated using the DEM coupled with computational fluid dynamics (CFD) and empirical studies by employing instruments such as conductivity probes to make load shape more realistic. Of course, some research has been done in this area. These researches' results demonstrate that the crescent shape of the active charge needs a bit of modification (Cleary et al., 2006; Mayank et al., 2015, Sinnott et al., 2017, Jahani Chegeni, 2019; Lvov and Chitalov, 2021). In future studies, it is necessary to include the results of these studies in the Morrell C-model. Another significant Morrell C-model drawback is ignoring the lifter design's effect on the power draw. Indeed, through its impact on the trajectories of balls falling, mixing the grinding media and slurry, and the level of charge vibration, the lifter design has a significant effect on the charge's dynamic inside the mills and, consequently, power consumption. Using both empirical and DEM studies, the effect of lifter design on the power draw can be examined. As a result, the lifter design's impact can be encompassed in the Morrell C-model by defining a lifter function.

Rajamani et al. (2019) used several industrial tumbling mills' net power data to assess the predictive capability of Hog and Fuerstenau's model. The results are shown in Fig. 6e. Although some errors are observed between the predicted and actual data, it can be concluded that there is a somehow acceptable agreement between them, particularly for ball mills. For this reason, the Moly-Cop tools, which have been provided to assess grinding media performance at a full industrial scale, use Hogg and Fuesrtanua's model to estimate the ball and SAG mills' net power draw (Molycop, 2021). However, it seems that this equation could be modified to predict SAG mills' net power consumption more precisely. For example, Doll (2016) found that, for calibrating Hog and Fuerstenau's model, the charge's angle of repose ("α") is affected by the aspect ratio of the mill and must be greater than the values supposed by Hog and Fuerstenau. Literature shows that the charge's angle of repose in cylindrical vessels is affected by various parameters, such as the angle of internal friction, particles' size and shape, density, moisture content, interface friction angle, and stratification (Hamzeh et al., 2018). However, there are no studies to determine the relationship of the charge's angle of repose with the mentioned parameters. The establishment of such a relationship through laboratory and simulation studies can lead to a more accurate charge's angle of repose and thus strengthen Hog and Fuerstenau's equation. Furthermore, like the Morrell C-model, the mentioned issues regarding lifter design and the grinding media dynamic voidage must be examined for the improvement of Hog and Fuerstenau's equation.
Daniel et al. (2010) tested the performance of Hogg and Fuerstenau's model, Austin's model, the Morrell C-model, the Morrell E-model, and the JKSimmet SAG mill model in predicting the pinion power of an industrial SAG mill. The results are shown in Fig. 6f. As can be seen, the models' output is more similar under SAG mills' normal operating conditions (fractional speed of 74 to 80 % and fractional filling of 14 to 18 %). But, the models' output deviation is visible in slower fractional speed or lower ball loads. As a result, it is suggested that the models' average results be used to determine power when non-standard mill operating conditions are specified. Given that in the actual conditions, the SAG mills' fractional filling by balls can be less than 14% (even about 7%), We believe it is necessary to calibrate the valid models such as Hog and Fuerstenau's equation and Morrell C-model by considering this issue.

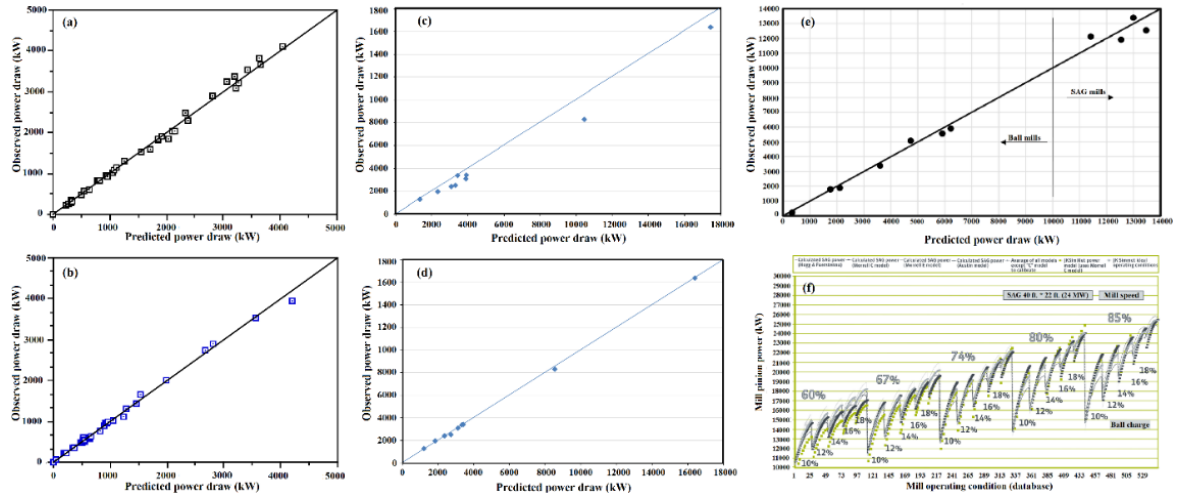

Fig. 6. Mill power equations' Performance. (a) Ball mills' predicted power by the Morrell C-model, (b) AG/SAG mills' predicted power by the Morrell C-model (Morrell, 1993), (c) SAG mills' predicted power by the Morrell C-model by assuming there is no slurry pool ($\theta_{TO} = \theta_T$), (d) SAG mills' predicted power by the Morrell C-mode by estimating θ_{TO} based on the progressive occupation of voidage by slurry (Morrell, 2016), (e) Performance of Hogg and Fuerstenau's model in predicting the mills' power draw (Rajamani et al., 2019), (f) Outputs of different power equations for a 40 × 22 ft. SAG mill (Daniel et al., 2010)

Overall, it can be concluded that the most crucial advantage of fundamental models over empirical models is paying attention to the charge motion. Moreover, making a relationship between mills' power draw and the parameters affecting it using physics laws is another advantage that validates these models over a broader range of operating conditions than empirical models. Although the influence of pulp rheology, pulp lifter performance, feed size distribution, slurry pool, and ore's hard components

building-up has been considered in these models, there are still shortcomings relating to their accurate effects. Besides, these models have not included other parameters such as lifter geometry, the realistic grinding media voidage, the shape of grinding media and feed particles, and particle size distribution of feed and grinding media. Furthermore, the energy consumption resulting from the heat generation due to friction, attrition, and abrasion breakage of the rock charge and rotational motion of the grinding media have not been accurately incorporated in the models because they are not adequately understood. Researchers can use two investigations conducted by Marino-Salguero et al. (2017) and Bouchard et al. (2018) in this field to calibrate the models. Indeed, the heat losses corresponding to the mentioned phenomena can be detected by tracing three heat flows: radiation and convention around mill shell, enthalpy flows with air, and enthalpy flows with slurry. We think that the enthalpy flows with slurry can be determined by tracing the mill's inlet and outlet pulp temperature difference through embedding temperature transmitters into the mill feed hopper and discharge sump. Accordingly, an empirical model can be derived to determine the slurry heat losses with respect to various conditions, including rotating speed, ore's abrasion, work index, and fractional filling. Moreover, thermography camera data can be used to trace radiation and convention around the mill shell.

2.2.2. DEM

In the last two decades, the discrete element method, has contributed to modelling the grinding and understanding the vague issues regarding this process. Indeed, there are some shortcomings in the other approaches in providing a realistic description of charge behaviour and predicting the power draw by changing the liner/lifer geometry, grinding media size distribution, feed size distribution, and pulp lifter geometry. This is where the DEM can be a facilitator through its superiority in modelling the individual motion of particles. While in other approaches, the whole mill charge is assumed as a locked mass. Fig. 7 demonstrates that the DEM has an outstanding ability to simulate the charge's shape inside mill at both subcritical and supercritical speeds (Govender et al., 2015). This section reviews the DEM's procedure in power draw prediction, the capabilities of both 2 and 3 dimensional DEM, the DEM's performance in predicting the full-scale mills' power draw, and DEM studies on the effects of mechanical components and operating parameters on power draw.

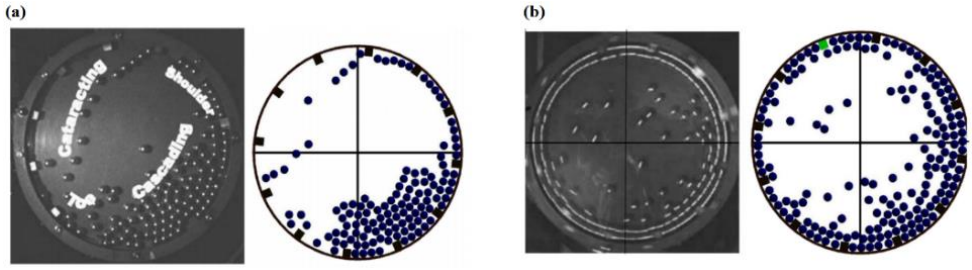

Fig. 7. The DEM predicted vs. actual shape of the charge (a) For fractional mill filling of 0.25 and mill rotating speed N=70 % of critical speed, (b) For fractional mill filling of 0.35 and mill rotating speed N=160 % of critical speed (Govender et al., 2015)

2.2.2.1. The DEM's procedure in the power draw prediction

Numerical modelling with taking advantage of the DEM was first used by Candall and Strack (1979) in soil mechanics. Mishra and Rajamani (1991) utilized the DEM to simulate the load behaviour in a ball mill and found that it can significantly influence designing and optimizing the milling process. The DEM uses two basic physics laws to model collisions of materials: force-displacement law and Newton's second law. A short contact between the particles leads to a collision causing the particles to overlap (see Fig. 8a), which DEM uses as particle's displacement. The DEM traces all displacements of discrete elements resulting from collisions and then models the forming new collisions for a period of t to $t+\Delta t$ called cycle time step by using calculation cycles. After conducting every cycle, the new momentary forces for each particle are calculated through force-displacement law. Next, the linear movement and each particle's speed are determined using Newton's second law. This calculation process is repeated for each cycle time step (Misra and Cheung, 1999; Weerasekara et al., 2013; Harvig, 2017).

During particles collision, in addition to the acceleration of gravity, another acceleration is applied to particles because of contact force. Hence, the DEM calculates particles' new velocity based on further acceleration. The contact force between two particles that causes them to overlap is defined by vertical and tangential components (see Fig. 8a). In the process of simplifying the calculation cycles, the contact force between two particles having a linear or non-linear relationship with the particles' overlap (Δx) is simulated based on the spring-slider-dashpot model (see Fig. 8b). The linear-spring dashpot model is the simplest type of contact model so that a constant value is considered for spring stiffness. By applying Hertz's theory, the linear model has been modified to incorporate the force deformation relation due to particles' body tending to deform; thus, the nonlinear-spring dashpot model has been developed (EDEM 2.6 User Guide, 2011). In the DEM calculation logic, the contact force and its tangential and normal components are calculated using the following equations (EDEM 2.6 User Guide, 2011):

$$F=F_n+F_t \tag{23}$$

$$F_n=-K_n\Delta x_n+ C_nV_{n_{rel}} \tag{24}$$

$$F_t=-K_t\Delta x_t+ C_tV_{t_{rel}} \quad \text{if} \quad F_t \geq \mu F_n \text{ then } F_t= \mu F_n \tag{25}$$

where F_n and F_t are the normal and tangential components of contact force, respectively, C and K are the functions of damping and stiffness, respectively, V_{rel} is the relative impact velocity, Δx is the particles' overlap, and μ is the friction coefficient. The subscripts n and t denote normal and shear direction at the contact point.

In the DEM, in the light of calculating the relative velocity and the contact force in both normal and tangential direction through Equations 23 and 25, the four following methods are used to predict the power draw through calculation of energy or torque consumption of tumbling mills:

A. Calculation of the energy lost (Datta et al., 1999): In the milling operation, the energy required for the charge motion is consumed in collisions and frictions. Some energy value is lost at each inelastic contact, represented by the dashpot in the spring-slider-dashpot model. Therefore, the energy lost at each contact is given by the integral of forces on the dashpot with respect to the displacement over a whole collision time as follow: (Datta et al., 1999; Tavares, 2017):

$$E= E_{dn}+E_{dn}= \int_0^{t_{contact}} F_{dn}dx_n + \int_0^{t_{contact}} F_{dt}dx_t \tag{26}$$

where F_{dn} and F_{dt} are the normal and tangential components of force on the dashpot (N), respectively, and dx is the particles overlap (m).

B. Calculation of the produced collision kinetic energy (Kwan et al., 2005; Wang et al., 2020): Based on calculating the displacement and velocity of particles using Newton's second law, the total milling's kinetic energy (E) can be given through total collision kinetic energy as follow:

$$E= \sum_{j=0}^{n} \frac{1}{2} mV_{rel}^2 \tag{27}$$

where m is the reduced mass of two involved particles in a contact $\left(\frac{2m_im_j}{(m_i+m_j)}\right)$ in kilograms, V_{rel} is the relative normal velocity of particles (m/s), and n is the total number of collision in each time step.

C. Calculation of the maximum contact energy (Wang et al., 2012): The DEM has employed the maximum impact energy, which specifies the maximum experienced stress by the involved particles in a collision, to estimate the total collision energy. When the maximum stress occurs in contact between two particles, the overlap reaches its maximum, and thus the maximum impact energy (E) is given by the integral of normal force and displacement as follow:

$$E= \int_0^{\Delta x_{n\ max}} F_n dx_n \tag{28}$$

where F_{dn} is the contact force's normal component (N) and dx is the particles' overlap (m).

By estimating the energy of all collisions during the total considered milling time in DEM simulation and using one of the methods mentioned above (Eq.s 26 to 28), the power draw is given by the basic power equation (Eq. 10).

D. Calculation of torque (Nierop et al., 2001): Calculating the torque resulting from a collision between grinding media and mill liner/lifters is another method used by DEM to predict the power draw. For contact between any mill lifter or liner element and a particle, the created torque in contact can be assessed by estimating the normal and tangential components of contact force and the distance from the mill's

center. Subsequently, the power draw is calculated through the torque-arm approach's basic equation (Eq. 11).

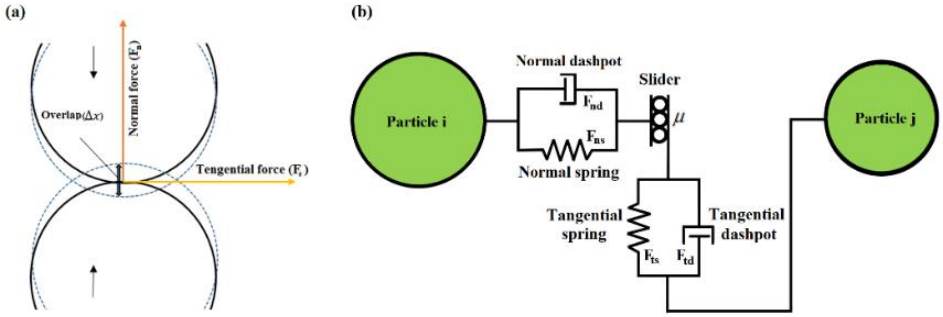

Fig. 8. The collision theory employed by DEM. (a) A simple illustration of the collision of particles (Johnson, 1985), (b) the spring-slider-dashpot model for a collision of two particles (Zhu et al., 2019)

In general, in the DEM calculation logic, after calculating the various possible contact forces inside a mill consisting of particle-particle, particle-lifter, and particle-liner forces, the particles' velocity and position are calculated through Newton's second law. Subsequently, using one of the four above mentioned methods, the power draw is calculated.

2.2.2.2. Comparison of 2 and 3 dimensional DEM in modeling of mill power draw

Numerous studies have been published relating to analysing the power draw of tumbling mills using two and three-dimensional DEM. In the 2D codes, the mills are modelled as a 2D circular slice of a mill with a width equal to the largest particle's diameter, while in the 3D codes, the collisions can be modelled for the entire mills' length (Rajamani et al., 2019). Since the 3D method was developed later, most modelling of tumbling mills has been conducted using 2D codes. On the other hand, the computational time limitation is another crucial reason for much research on the 2D method.

The literature shows that the performance of 3D codes in modelling the power draw of both industrial SAG and ball mills is more accurate than 2D codes (Venugopal and Rajamani, 2001; Kimura et al., 2007; Rajamani et al., 2019). This can be clearly seen in Table 1, which is the results of an evaluation study conducted by Rajamani et al. (2019). This prediction accuracy is attributed to the 3D codes' capability to simulate millions of particles with millions of collisions and incorporate the effect of feed characteristics and discharge lifters in the power calculation. Furthermore, the 3D codes can precisely estimate the position of the shoulder and toe and the trajectory curves that can be different in the length direction of the mill. In contrast, in the 2D codes, only the behavior of a slice of the length that cannot represent the entire mill length is considered to calculate the power draw. However, the main disadvantage of the 3D codes is the computational time limitation. In such simulations, millions of particles' collisions are followed to calculate the system's collision energy, which requires intensive computational for the code execution. It should be mentioned that the advances in Graphical Processor Unit (GPU) computing codes have made it more facilitative to do such tasks. However, using this advanced GPU to predict the power draw increases the price of computer hardware considerably (Peng et al., 2016).

Table 1. The DEM prediction results vs. actual power draw of industrial tumbling mills (Rajamani et al., 2019)

Mine site	Mill type	Mill dimension (ft.)		Fractional speed (%)	Fractional mill filling (%)	Net power (MW)		
		Diameter	Length			Actual	Predicted by the DEM (2D codes)	Predicted by the DEM (3D codes)
Constancia	SAG	36.00	26.50	72.00	26.00	13.7-	14.1	14.3
Constancia	Ball	26.00	40.50	74.00	32.00	13.4	12.9	13.1
Tongon	Ball	20.00	32.00	75.00	33.00	8	7.2	7.5

2.2.2.3. DEM's performance in predicting the full-scale mills' power draw

This section shows the DEM's capability in the prediction power of both ball mills and SAG mills. Fig. 9 illustrates the proper predictive capability of DEM in predicting the net power draw of ball mills for a wide range of diameter (Detta et al., 1999). The presented data in Table 1 and Fig. 9 prove that summing the energy loss in the individual collisions during grinding, which is the basis of power calculation in the DEM, is a reliable approach to predicting the mills' net power draw.

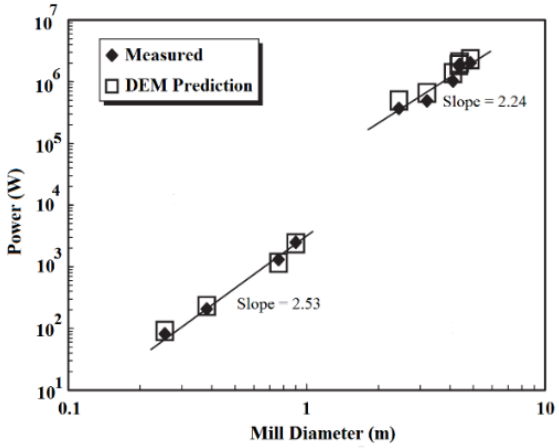

Fig. 9. DEM prediction results vs. actual power draw of ball mills (Datta et al., 1999; Mishra, 2003)

Table 2 demonstrates a comparison between the Morrell C-model and the 3D DEM in predicting the gross power of an industrial SAG mill in two different scenarios. As can be seen, the prediction of both models is less than the actual value, although the Morrell C-model has predicted the power more accurately. Likewise, Fig. 10 illustrates an industrial AG mill's actual gross power draws versus predicted values by both the Morrell C-model and the 3D DEM (CMD consulting, 2021). As depicted, at high powers, the predicted powers by the DEM are significantly less than the Morrell C-model. The main shortcoming of DEM leading to the under-estimation of gross power is the neglect of energy losses in the motor, gearbox, and bearing. This issue should be considered in the DEM's future progression to make it applicable in designing, monitoring, and controlling tumbling mills' circuits compared to the Morrell C-model. Furthermore, the computational time limitation is another DEM's shortcoming that restricts this method for more realistic simulation of particles' collisions (Marrison et al., 2001; Govender et al., 2015). The challenge of modelling fine particles is another major shortcoming of DEM because the grinding environments include trillions of fine particles. It becomes computationally impossible to account for every individual real-sized particle. While, in real industrial mills, fine particles will cushion impacts between large ones, affecting the amount of impact force and, consequently, power draw.

Table 3 presents a comparison between the DEM and the Morrell C-model in predicting the gross power of an AG mill in two different conditions, including with and without the slurry pool (CMD consulting 2021). As can be seen, the DEM could not consider the slurry pool's effect. In comparison, the Morrel C-model determines the mill's power in the presence of the slurry pool correctly less than in its absence. It is important to note that to achieve a more realistic description of charge motion by considering the influence of the slurry medium, investigators have employed coupling of DEM and

Table 2. Comparison of the DEM and the Morrell C-model in predicting the power draw of a SAG mill with a size of 5.26*10.86 m (Marrison et al., 2001)

Case	Parameters					Power draw (kW)		
	Lifters' number	Ball top size (mm)	Ball load (%)	Total load (%)	Fractional speed (%)	Operating	Predicted by Morrell C-model	Predicted by DEM
1	72	125	11	26	80.4	12711	11501	9842
2	48	150	12	21	74	10800	10500	9563

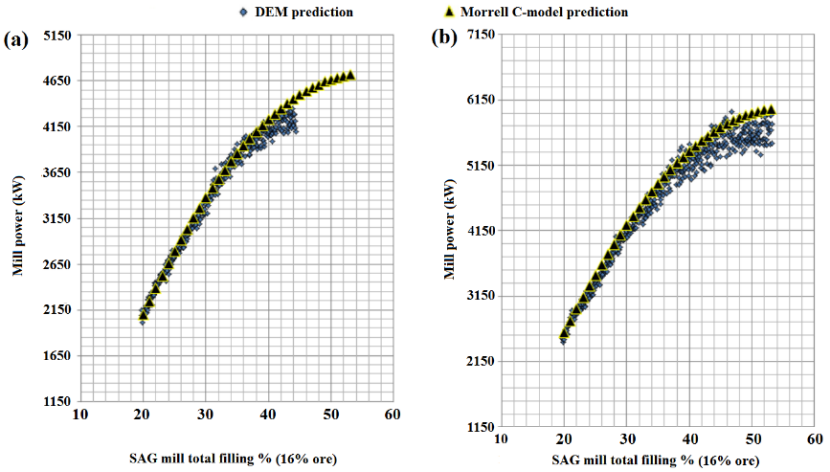

Fig. 10. Comparison between the DEM and the Morrell C-model in predicting the power of a SAG mill with a size of 5.9*11.1 m. (a) For rotating speed N=62 % of critical speed, (b) For rotating speed N=75 % of critical speed (CMD consulting, 2021)

other techniques such as smoothed particle hydrodynamics (SPH) or computational fluid dynamics (CFD). These researches' results revealed that by employing the CFD or SPH methods coupled with the DEM, the energy consumption could be estimated more precisely because of accounting for the fluideffect (Cleary et al., 2006; Mayank et al., 2015, Sinnott et al., 2017, Jahani Chegeni, 2019; Lvov and Chitalov, 2021). However, some key challenges must be solved in the future DEM application coupled with CFD or SPH, including; the influence of fine particles between the colliding elements, the effect of slurry density and viscosity, modelling the grinding process continuously, and the impact of realistic particle shapes.

With all of the above mentioned, the DEM modelling is a suitable platform for advancing understanding power draw in tumbling mills' operation. However, it still needs to evolve and progress for future milling equipment control and design.

Table 3. Comparison between the DEM and the Morrell C-model in considering the effect of slurry pool in predicting the grate discharge mills' power draw (CMD consulting, 2021)

Model	Parameters					Power draw (kW)	
	AG mill's length (m)	AG mill's diameter (m)	Total load (%)	Fractional speed (%)	Ore specific gravity (tonnes/m3)	With slurry pool	Without slurry pool
DEM	11	11.1	40	60	2.7	2800	2800
Morrell C-model	5.9	11.1	40	60	2.7	2545	2059

2.2.2.4. DEM investigations on factors affecting the power draw of tumbling mills

Many vague issues regarding the effect of different parameters on the power draw have been investigated using the DEM. This section tries to provide a comprehensive review of DEM investigations on parameters affecting the tumbling mills' power draw.

2.2.2.4.1. Mill diameter, rotating speed, and fractional mill filling

The mill diameter, rotating speed, and fractional mill filling as the most prominent affecting parameters of the mill's power draw have been investigated by DEM in various studies. (Cleary, 2001; Datta et al., 1999; Djordjevic, 2004; Kime, 2017; Yin et al., 2017; Maleki Moghaddam et al., 2018). As illustrated in Fig. 9, there is an acceptable agreement between DEM predicted, and actual power draws in the different diameters. Besides, the best-fit line's slope is equal to 2.53 and 2.24 for laboratory and industrial scale, respectively, around the Bond exponent of 2.3 (Bond, 1962).

Bond (1961) experimentally found that the maximum power draw occurs at 94% of critical speed. Yin et al., 2017, indicated that this phenomenon occurs because the number of collisions reaches its maximum at mentioned speed. Likewise, the DEM simulation results demonstrate that the maximum power draw occurs at about 90 % of critical speed (see Fig. 11a), close to Bond's proposed value (94%). Bond (1961) empirically found that the maximum power draw occurs when the fractional mill filling reaches 53 %. Fig. 11b illustrates that in the DEM simulation results, the maximum power consumption occurs at the same mill filling. According to Equation 12, the power draw functions the charge weight and the lever arm distance. Although the charge weight increases with increasing the fractional mill filling, the lever arm distance decreases, making the power draw's trend bell-shaped.

2.2.2.4.2. Liner and lifter geometry

Sacrificial liners equipped with lifters are mounted onto the mill shells, not only for protecting the mill shells from high wear rate but also for increasing the grinding efficiency by enhancing the fraction of cataract load for reaching the maximum impact breakage energy. Accordingly, the effect of the lifter's number and characteristics, including shape, height, and face angle on the mills' power draw, has been investigated using the DEM (Datta et al., 1999; Cleary, 2001; Djordjevic, 2003; Djordjevic et al., 2004; Kime, 2017; Bian et al., 2017; Yin et al., 2017; Yin et al., 2018; Kolahi and Jahani Chegeni, 2020).

Fig. 11c illustrates the lifter face angle's effect on an industrial mill's power draw per charge tonne. As depicted, the power draw decreases gradually as the lifter face angle increases. This is attributed to the load behaviour so that more grinding media are projected into the cataract region by increasing the face angle. Likewise, the same results were reported by Hlungwani et al. (2003) and Kime (2017).
The impact of lifter shape could be explained similarly to the presented reason for the lifter face angle. Datta et al. (1999) found that the power draw has the maximum value for the rectangular lifter (see Fig. 11d), attributed to the interaction of the bigger face angle of this lifter and the mill's rotation speed. Yin et al. (2018) investigated the ball mill's power draw with different lifter shapes, including rectangle, waveform, and trapezium, and concluded that the trapezium lifter draws the maximum power. In another research, Jahani Chegeni et al. (2020) examined an industrial SAG mill's energy consumption with three different liner geometry named Wave, Rib, and Osborn. They concluded that the energy consumption is maximum in using the Osborn liner, attributed to edged lifters.

The lifters' height and number are other important parameters that have been examined by various researchers (Datta et al., 1999; Djordjevic et al., 2004; Kime, 2017; Bian et al., 2017; Kolahi and Jahani Chegeni, 2020). Fig. 11e illustrates the DEM results of the lifter height effect on a ball mill power draw.

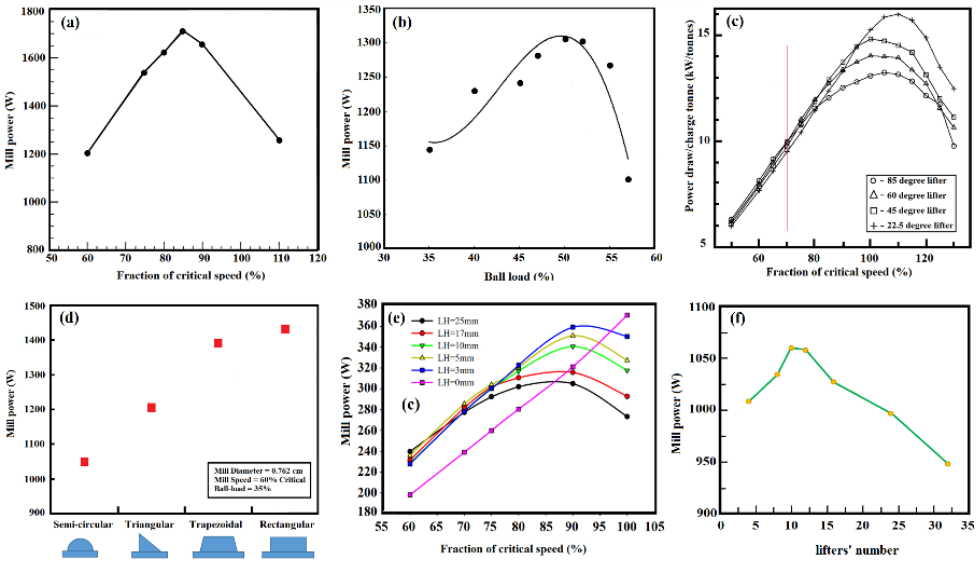

Fig. 11. The DEM simulation result regarding the effect of operating parameter on the mill power draw. (a) Effect of rotation speed, (b) Effect of fractional mill filling (Datta et al., 1999). (c) The impact of lifter face angle (Cleary, 2001), (d) The effect of lifter shape (Datta et al., 1999), (e) The effect of lifter height (Yin et al., 2017), (f) The effect of lifter number (Datta et al., 1999)

As depicted, the maximum power occurs for the higher lifters at low mill speeds. Conversely, at high rates, the maximum power occurs for the shorter lifters, attributed to increasing movement and lifting the balls at low speeds and increasing the centrifuge layer thickness at the high rates (Kolahi and Jahani Chegeni 2020). The effect of lifters' number on the mill-power has been reported similar to lifter height's impact. The extent of cataract motion and, subsequently, power draw will be significantly enhanced as the lifter number increase to a specific limit, as shown in Fig. 11f (Datta et al. 1999). Therefore, the power draw passes through the maximum and decreases because of trapping grinding media between lifters, which behave like a mill with less volume (Yin et al. 2017).

2.2.2.4.3. Pulp lifter Geometry

With respect to Equation 22, the pulp lifter's performance has a remarkable effect on the power draw. Literature indicates that the pulp lifter mechanism leads to lower discharge than when the grate discharge system is used. This is due to the inherent defects in ordinary pulp lifter systems design, allowing a proportion of pulp flow back into the mill before discharge through mill trunnion, which may cause the formation of a slurry pool and thus reduce the power draw and grinding efficiency. Hence, the effect of pulp lifter characteristics, including depth, the vans' number, and the type of lifter assemblies consisting of straight, curved, or twin-chamber on the power draw, have been investigated using DEM (Royston, 2000; Royston, 2005; Latchireddi, 2002; Latchireddi and Morrell, 2003; Chu, 2011; Gutiérrez et al,. 2019). However, the effect of pulp viscosity and PSD of mills' product on the pulp lifter's performance and power draw has not yet been examined, which needs to be investigated using DEM coupled with CFD or SPH in future investigations.

2.2.2.4.4. The shape of grinding media and feed particles

Since the particles' shape has a significant effect on the mill charge's dynamics and achieving its data is difficult because of the milling's harsh environment, the DEM has been applied to analyze its effect on the power draw. Although some laboratory studies have been conducted on the effect of grinding media's shape (Lameck, 2005; Simba, 2010; Khumalo et al., 2019; Shahbazi, 2020), it has not been incorporated in power equations.

Kiangi et al. (2013) investigated the effect of different grinding media shapes on the power draw of a pilot-scale mill by application of the DEM and concluded that the power draw could be described in the following order for different media shapes: worn balls>spheres>cylpebs. The same results were reported in the emprical research conducted by Lameck et al. (2006). Weerasekara et al. (2016) employed round and clumped balls to study the total energy dissipation of ball mills and found that collision energy's tangential components using rounded balls are significantly less than clumped ones. In another research, Govender et al. (2018) examined the power draw of a laboratory-scale mill in different grinding media shapes and concluded the maximum and minimum value of power draw occurs for the truncated tetrahedron and sphere, respectively (see Fig. 12). Although grinding media shape's importance lies in three reasons, including their deformation during milling operation, the existence of various grinding media shapes,s and their remarkable effect on the mill charge's dynamics, few articles have been published examining its effect on the mill power draw. Since the shape of the grinding media changes under the influence of factors including impact, attrition, corrosion, and chipping, we recommend that the effect of a realistic combination of grinding media's shapes on the power draw be studied. By draining the balls from inside a ball mill during a mineral processing plant overhaul, the actual shape distribution of grinding media can be determined and then modeled using the DEM.

It is well known that the feed characteristics such as particle shape, angularity, and aspect ratio have notable influences on the AG/SAG mill's performance (Cleary and Owen 2019; Tavares et al. 2020). Hence the feed particles' shape effect on the power draw has been considered in DEM's investigations.

Tavares et al. (2020) adopted a new breakage model in DEM modelling using the polyhedral particles, which are more similar to actual rock shapes. They found that the DEM using polyhedral particles could more accurately describe the ore's size distribution resulting from breakage in grinding and consequent energy consumption. Cleary and Owen (2019) investigated the impact of rock shape on

an industrial SAG mill's power draw by applying 3D DEM. They found that the power draw is persistently higher for the non-spherical particles, attributed to the higher shoulder and toe positions than spherical particles. Moreover, they observed that the difference in power draw for these two cases declines with increasing the mill rotating speed but enhances with decreasing the lifter height and increasing the fractional mill filling and the rock to ball ratio.

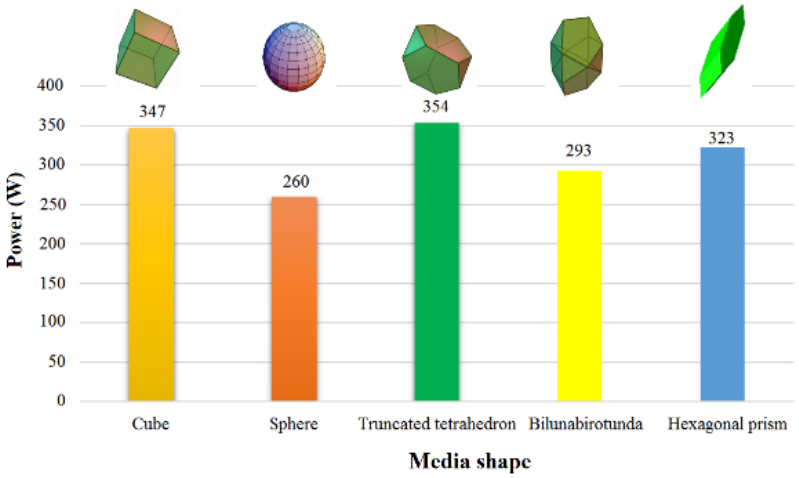

Fig. 12. The DEM simulation result regarding the effect of grinding media shape on the power draw (Govender et al., 2018)

2.2.2.4.5. The grinding media and feed particle size distributions

A wide range of impact forces must be created inside a mill for optimum grinding, achieved by selecting the suitable ball size distribution (BSD). To this end, Bond's method is used to determine an appropriate BSD for the mills' first filling (Bond, 1958). Many researchers have studied the BSD's effect on mills' power draw (Bond, 1961; Austin et al., 1976; Djordjevic, 2005; Katubilwa et al., 2009; Magdalinovic, 2012; Cho et al., 2013; Zhang et al., 2014; Kabezya et al., 2015). Since the BSD's effect has not been considered in the power equations, some attempts have been made to assess its impact by utilizing the DEM.
Djordjevic (2005) investigated the impact of BSD on the net power of a 5 m diameter ball mill. He found that, for a given BSD, the power draw will be decrease with a slight trends by replacing the smallest balls with bigger ones; and after passing through a certain size, a significant reduction in power draw is observed (see Fig. 13a). Panjipour and Barani (2018) examined the BSD's effect on the power draw of a laboratory ball mill in different fractional mill fillings and BSDs. This investigation's results demonstrate that for all values of fractional mill filling, the maximum power draw occurs when the percentage of small balls is between 30-40% (see Fig. 13b). Similarly, the same results have been reported by Amannejad and Barani (2020). Moreover, they reported that the rotating speed's effect on the power draw significantly depends on BSD. Although some attempts have been made to assess the BSD impact on the power draw by applying the DEM, there are still shortcomings in this regard. We recommend the Bond's proposed BSDs for ball mills' first filling at the commissioning stage be used to examine the BSD effect and find the optimum size of the make-up ball from the power draw point of view. Moreover, the realistic BSD, which can be obtained by discharging the balls during plants' overhaul, can be used as input data to more realistically trace BSD's effect on power draw.

According to Silva and Casali's model (Eq. 9), the effect of feed size distribution on the mills' power draw, particularly SAG mills, is remarkable. Nevertheless, few papers have been published in this regard. For instance, the DEM can contribute to upgrading Silve and Casali's model in terms of defining a function for intermediate size fraction (-6"+1" in the original model) based on operating and mill design parameters.

Kwan et al. (2005) studied the effect of feed particle size distribution (PSD) on a laboratory ball mill's power draw using the DEM. They reported that the power draw has a linear relationship with the feed PSD, and its maximum value corresponds to the largest size fraction, as illustrated in Table 4.

In another research, Weerasekara et al. (2016) investigated the effects of feed particle size distribution and mill diameter on the power draw of three pilot-scale SAG mills with different diameters. This study demonstrated that the smaller particles consume higher energy leading to higher mill's power draw; in contrast, the biggest ones consume less energy. Besides, they found that the average particles' energy consumption increases with an increase in mill diameter.

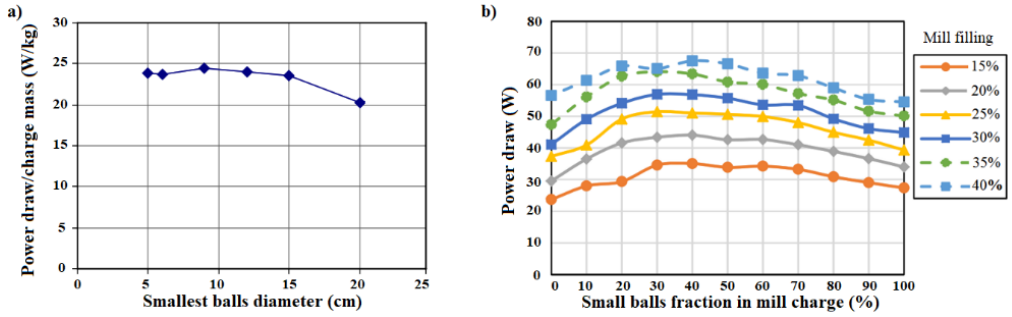

Fig. 13. The DEM simulation results. (a) The BSD's effect on the power of 5 m diameter ball mill (Djordjevic, 2005), (b) The mutual effect of the BSD and fractional filling on the power of a 25 cm diameter ball mill (Panjipour and Barani, 2018)

Table 4. The DEM result regarding the feed particle size's effect on a laboratory ball mill's power draw (Kwan et al. 2005)

Feed Size Range (μm)	Mean feed size (μm)	Predicted Power (JS^{-1})
500-600	550	83.93
425-500	463	70.58
355-425	390	59.51
250-300	275	41.97
212-250	231	35.25

3. Power consumption's optimization

The US. Department of Energy has reported that the most significant potential for energy-saving in all mining-related operations is to optimize grinding processes; because the energy efficiency of tumbling mills is considerably low (U.S. DOE, 2007). Hence, the manufacturers have attempted to improve the tumbling mills' components, such as the lubrication systems, the geared drives, and the electric motors. Furthermore, optimization of filling level and stability of rotating speed has been made by designers. One of the main dramatic problems resulting in the low energy efficiency of mills is that about 30 % of grinding bodies remain in a dead zone and are not involved in the dynamic process (Goralczyk et al., 2020). Thus, utilizing instruments that can provide data on dynamic phenomena inside the mills can update power draw models to increase energy efficiency by choosing the optimum operating parameters. In other words, the optimal condition and related power draw can be extracted from such models in which the maximum live grinding zone is achieved.

An investigated promising approach to utilizing the dynamic phenomena in increasing the grinding efficiency is making the oscillatory movement (resonance and synchronous) of the central part of material inside the mill against the mill shell so that the rest of the load is a passive part (Goralczyk et al., 2020). Since the electrical power draw of the largest mills is about 20 to 30 MW, even a tenth of a percent reduction of energy consumption provides a tremendous annual energy saving for mineral processing plants. Literature shows that by implementing the oscillation of material, which is occurred in a particular value of rotating speed and feed rate, the energy consumption can be decreased in the range of 8-10 % (Maryuta, 1993). The different instruments that nowadays are used by industrial technologists such as Mintek, Outotek, and FLSmith for the control of milling operation, can be utilized for implementing this approach as a suitable online process and condition monitoring tool. Most used measurements in industrial applications are based on electric motors' power, mills' rotating speed, acoustic emission, sliding bearing oil pressure, vibration, the torque of drives, vision, weightometer

(belt scale), particle size distribution analyzer, and slurry density meter (Maryuta, 1993; Outotec, 2020; FLSmidth, 2020). Based on this, the effect of the oscillatory phenomenon on the mill's power draw can be realized by indirect measurement of load dynamics with different physical nature signals. Campbell et al. (2001) showed that the multi-sensor surface vibration monitoring system can can sufficiently trace the level of the oscillatory movement inside the mills.

We believe that implementing a process control system in which the instrumentations' signals are collected and analyzed can upgrade the power draw models to optimize power consumption by considering the effect of oscillatory movement. We suggest the shown instruments in Fig. 14 for this program's future studies. The proposed control system utilizes a motor's signal for detecting the mill's gross power, a VFD's signal for detecting the rotating speed rate, a density meter's signal for detecting pulp density, a belt scale for detecting the ore's feed rate, a signal of PSD analyzer for determining product's particle size distribution, sliding bearing oil pressure transmitter signal for detecting the fractional mill filling, and vibration signal for detecting the level of oscillatory movement. From the results of the implementation of this program, the relationship between the level of oscillatory movement and power draw can de be determined in the various level of slurry density, mill rotating speed, fresh feed rate, and fractional mill filling. On the other hand, the PSD of the mill product can be traced. Since the optimum oscillatory increases the efficiency of the mill, it can be realized that at which level of vibration the feed rate can be increased so that the product's particle size distribution remains the same. In other words, such examination leads to an increase in the mill's capacity with lower specific energy consumption. Indeed, the efficient condition delivers the least specific energy to accomplish a particular size distribution of products. Based on this, an empirical model can be developed in which the power draw and value of operating parameters for achieving the optimum oscillatory level be derived. Moreover, it is recommended that the DEM be coupled with the experimental results to assist the interpretation of the oscillatory level signature.

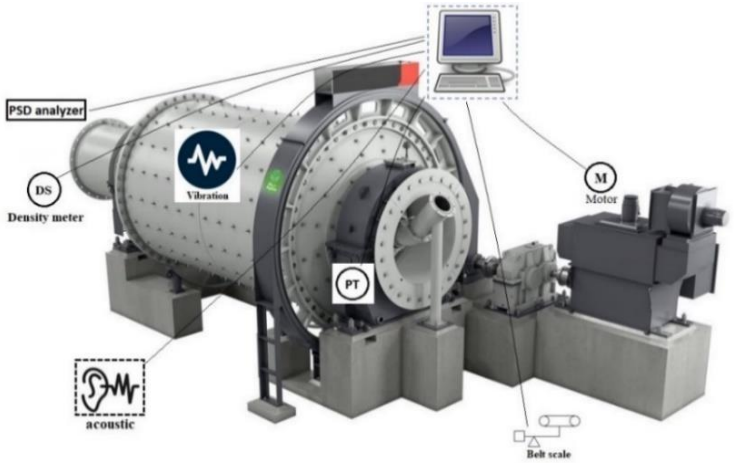

Fig. 14. The proposed approach for updating the power draw models in terms of increasing the mills' efficiency

4. Conclusions

A review article has been presented to examine the performance of tumbling mills' power models and the employed methods in their development, specify the effective parameters incorporated in them, identify their shortcomings, and suggest future studies. The literature demonstrates that researchers have made worthwhile efforts to integrate various parameters into the mils' power equations. Nevertheless, it seems that there still exists an array of gaps. In conclusion, the following issues were found which need to be investigated in future studies:

1. In all models, the grinding media voidage, vital in estimating the charge bulk density, is assumed static and equal to 0.4. However, even the static voidage depends on the grinding media's size distribution and shape. On the other hand, the mill charge has a dynamic state and varies by changing the operating parameters. Therefore, two issues need to be investigated in future studies:

- preparing an equation to determine the static voidage based on the grinding media's shape and size distribution.
- development of an equation to assess the impact of change in the fractional mill filling, grinding media's shape and size distribution, and the fractional speed on the dynamic voidage.

2. Since the shape of the grinding media changes under the influence of factors including impact, attrition, corrosion, and chipping, research on incorporating the effect of grinding media into the power equations by considering the realistic distribution of shape and size can be essential and efficient while was not yet investigated.
3. To upgrade the Hog and Fuerstenau's model, especially for SAG mills, the possibility of the development of an empirical model to determine the mill charge angle of repose with respect to the angle of internal friction, particles' size and shape, charge density, moisture content, interface friction angle, and stratification must be investigated.
4. There is little information on heat generation due to friction, attrition and abrasion breakage of the charge and its rotational motion. The heat losses during grinding can be detected by tracing radiation and convention around the mill's shell, enthalpy flows with air, and enthalpy flows with slurry. These can be determined using instruments such as temperature transmitters and thermography cameras. Accordingly, a mathematical model can be derived to determine the heat losses with respect to various conditions, including rotating speed, ore's abrasion and work index, fractional mill filling, etc.
5. By applying DEM, the effect of different ball size distribution, proposed by Bond for mill's first filling, on the power draw must be investigated to obtain the optimal ball size distribution. In this way, the optimal size of the largest ball charged to the mills can be achieved. Besides, the effect of BSD on the power draw can be included in models by defining an index like the mean absolute deviation of balls' diameter that can represent balls' BSD.
6. The effect of the ore abrasion Index, which can affect the mills' power draw by deforming the grinding media shape, changing the voidage value, and increasing grinding media consumption, shall be investigated.
7. There is lack of research about the effect of pulp viscosity and mills' product PSD on the pulp lifter's performance and power draw, which needs to be investigated using DEM coupled with CFD or SPH.
8. Since the lifter design has a significant impact on the charge's dynamic inside the mills and consequently power consumption, it is required the lifters desgin be incorporated into into the modified Morrell C-model by defining a lifter function using both empirical and DEM studies.
9. The tumbling mills' power draw has not been studied using various feeds with the same size distribution but different F_{80} values, which the DEM can carefully examine. Such investigation can be very efficient and helpful in optimizing SAG mills' feed size distribution through adjusting the feed rate of apron or vibrating feeders installed in stockpiles.
10. Silva and Casali's model applies the -6"+1" fraction of feed as the intermediate size fraction affecting SAG mill power. Given that the impact mechanism is dominant in SAG mills and the amount of power consumption is associated with ore's Bond work index, we think that the intermediate size fraction may vary for different minerals and SAG mill's diameters. Hence, this issue must be investigated to upgrade Silva and Casali's model.
11. There is a lack of research regarding power draw optimization, which needs to be investigated through pilot-scale tests using a process control system comprised of different instruments, data acquisition, and analyzing systems. For instance, the effect of the oscillatory movement on the power draw optimization can be examined through the proposed control system in Fig. 14.
12. The most critical work for the future is employing the DEM outputs for improving the valid power models. For instance, the lifter geometry and grinding media and particles' shape has not been included in the Morrell C-model, which can be implemented by defining functions based on the DEM's outputs.

Overall, it is concluded that the power models could be more efficient and applicable if the identified shortage items in this paper are investigated, and their effects are included in the models.

References

AMANNEJAD, M., BARANI, K., 2020, *Effects of ball size distribution and mill speed and their interactions on ball milling using DEM*. Mineral Processing and Extractive Metallurgy Review, 1-6, doi: 10.1080/08827508.2020.1781630.

AUSTIN, L. G., 1990, *A mill power equation for SAG mills.* Mining, Metallurgy & Exploration, 7, 57–63.

AUSTIN, L. G., SHOJI, K., LUCKIE, P. T., 1976, *The effect of ball size on mill performance.* Powder Technol, 14, 71–79.

BASIRIFAR. F., BAHRI, Z., ABOLHASANI, M., NASERI. S., 2018, *A comparison of power draw models in predicting the power of wet ball mill, a case study of Iran Alumina Co.* 9th Iranian Mining Engineering Conference, Tehran, Iran, 542-546. (In Persian)

BIAN, X., WANG, G., WANG, H., WANG, S., LV, W., 2017, *Effect of lifters and mill speed on particle behaviour, torque, power consumption of a tumbling ball mill: Experimental study and DEM simulation.* Minerals Engineering, 105, 22–35.

BOND, F.C., 1958, *Grinding ball size selection.* British Chemical Engineering, 16, 378–385.

BOND, F.C., 1961, *Crushing and grinding calculations.* British Chemical Engineering, 16, 543–548.

BOND, F.C., 1962, *Additions and revision to crushing and grinding calculations.* Allis Chalmers Publication.

BOUCHARD, J., LEBLANC. G., LEVESQUE, M., RADZISZEWSKI, P., GEORGES-FILTEAU, D., 2019, *Breaking down energy consumption in industrial grinding mills,* CIM Journal, 10.

BUENO, M. P., KOJOVIC, T., POWELL, M.S., SHI, F, 2013, *Multi-component AG/SAG mill model.* Minerals Engineering, 43, 12-21.

CANDALL P. A. AND STRACK, O. D. L., 1979, *A discrete numerical model for granular assemblies.* Géotechnique, 29, 47-65.

CAMPBELL, J., SPENCER, S., SUTHERLAND, D., ROWLANDS, D., WELLER, K., CLEARY, P., ADRIAN HINDE, A., 2001, *SAG mill monitoring using surface vibrations,* SAG 2001 Third International Autogenous and Semiautogenous Grinding Technology, Vancouver, B.C., Canada,373-385.

CHO, H., KWON, J., KIM, K., MUN, M., 2013, *Optimum choice of the make-up ball sizes for maximum throughput in tumbling ball mills.* Powder Technology, 246, 625-634.

CHU, P., 2011, *Discrete element method modeling of pulp lifter performance.* Master thesis, Department of Mechanical Engineering, McGill University.

CLEARY, P. W., 2001, *Charge behavior and power consumption in ball mills: sensitivity to mill operating conditions, liner geometry and charge composition.* Int. J. Miner. Process. 63- pp. 79–114.

CLEARY, P., OWEN, P., 2019, *effect of particle shape on structure of the charge and nature of energy utilization in a SAG mill.* Mineral engineering, 132, 48-68.

CLEARY, P.W., SINNOTT, M., MORRISON, R., 2006, *Prediction of slurry transport in SAG mills using SPH fluid flow in a dynamic DEM based porous media*, Minerals Engineering, 19, 1517–1527.

CMD CONSULTING, 2021, https://www.cmdconsulting.com.au/

DANIEL, M., LANE, G., MORRELL, S., 2010, *Consolidation and validation of several tumbling mill power models*. PROCEMIN 2010, Santiago, Chile, 84-92.

DATTA, A., MISHRA. B. K., RAJAMANI, K., 1999, *Analysis of power draw in ball mills by the discrete element methosd.* Canadian metallurgical quarterly, 38, 133-139.

DAVIS E.W., 1919, *Fine crushing in ball mills.* AIME Transactions, 61, 250 -296.

DJORDJEVIC, N., 2003, *Discrete element modeling of the influence of lifters on power draw of tumbling mills.* Minerals Engineering, 16, 331–336.

DJORDJEVIC, N., 2005, *Influence of charge size distribution on net-power draw of tumbling mill based on DEM modeling.* Minerals Engineering, 18, 375–378.

DJORDJEVIC, N., SHI, F. N., MORRISON, R., 2004, *Determination of lifter design, speed and filling effects in AG mills by 3D DEM.* Minerals Engineering, 17, 135–142.

DOLL, A. G., 2016, *An updated data set for sag mill power model calibration.* XXVIII International Mineral Process Congress, Quebec, Canada, 1-22.

ERDEM, A. S., ERGUN, S. L., BENEZER, A. H., 2004, *Calculation of the power draw of dry multi-compartment ball mills.* Physicochemical Problems of Mineral Processing, 38,221-230.

FUERSTENAU, D. W., KAPUR, P.C. AND VELAMAKANI B., 1990. *A multi-torque model for the effects of dispersants and slurry viscosity on ball milling.* International Journal of Mineral Processing, 28, 81 -98.

FLSMIDTH. *Maximize Grinding Efficiency with LoadIQ*. Available online: https://www.kscape.com/loadiq (accessed on 23 May 2020).

GOVENDER, N., RAJ K. RAJAMANI, R. K., KOK, S., WILKE, D. N., 2015, *Discrete element simulation of mill charge in 3D using the BLAZE-DEM GPU framework.* Minerals Engineering, 79, 152-168.

GOVENDER, N., RAJ RAJAMANI, R. K., DANIEL N. WILKE, D. N., CHUAN-YU WU, C., JOHANNES KHINAST, J., GLASSER, B. J., 2018, *Effect of particle shape in grinding mills using a GPU based DEM code.* Minerals Engineering, 129, 71-84.

GUTIÉRREZ, A., AHUES, D., GONZÁLEZ, F., MERINO, P., 2019, *Simulation of Material Transport in a SAG Mill with Different Geometric Lifter and Pulp Lifter Attributes Using DEM.* Mining, Metallurgy & Exploration 36, 431–440.

GÓRALCZYK. M., KROT, P., ZIMROZ, R., OGONOWSKI, S., 2020, Increasing Energy Efficiency and Productivity of the Comminution Process in Tumbling Mills by Indirect Measurements of Internal Dynamics—An Overview, energies, 13, 6735.

HAMZAH, M., BEAKAWI, A., OMAR, S., BAGHABRA, A.,2018, *A review on the angle of repose of granular materials*, Powder Technology, 330, 397-417.

HARRIS, C. C., SCKNOCK, E. M., ARBITER, N., 1985, *Grinding mill power consumption.* Mineral Processing and Technology Review, 1, 297 - 345.

HARVIG, J., 2017, *On the Adhesive Behavior of Micron-sized Particles in Turbulent Flow*. PhD thesis, Department of Energy Technology, Aalborg University.

HLUNGWANI, O., RIKHOTSO, J., DONG, H., MOYS, M. H., 2003, *Further validation of DEM modeling of milling: effects of liner profile and mill speed.* Minerals Engineering, 16, 993–998.

HOGG, R., FUERSTENAU, D. W., 1972. *Power relationships for tumbling mills.* Trans. SME/AIME, 252, 418 - 423.

JAHANI CHEGENI, M., 2019, *Combined DEM and SPH simulation of ball milling, Journal of Mining and Environment (JME)*, 10, 151-161.

JAHANI CHEGENI, M., KOLAHI, S., NIKOUEI MAHANI, A., 2020, I*nvestigation and comparison of grinding media energy in SAG mills with different liners by Discrete Element Method.* 8th Iranian Mining Engineering Conference, 1-9. (In Persian)

JOHNSON, K. L., 1985, *contact mechanics*, Cambridge: Cambridge university press.

KABEZYA, K., MOTJOTJI, H., 2015, t*he Effect of Ball Size Diameter on Milling Performance.* J. Mater. Sci. Eng. 4, 4–6.

KATUBILWA, F. M., MOYS, M. H., 2009, "Effect of ball size distribution on milling rate." Miner. Eng, 22, 1283–1288.

KHUMALO, S., N. HLABANGANA, N., DANHA, G., MUZENDA, E., 2019, *Effect of media shape on particle breakage in a batch ball mill: Lessons learnt from Population Balance Model and Attainable Region technique.* SMPM 2019, Sun City, South Africa, 76-79.

KIANGI, K., POTAPOV, A., MOYS, M., 2013, *DEM validation of media shape effects on the load behaviour and power in a dry pilot mill*. Minerals Engineering, 46, 52-59.

KIME, M. B., 2017, *using the discrete-element method to investigate ball milling power draw, load behavior, impact energy profile.* CIM Journal, 8, 59-66.

KIMURA, M., NARUMI, M., KOBAYASHI, T., 2007, *Design Method of Ball Mill by Discrete Element Method*. Sumitomo Kagaku, 2, 1-9.

KING, R. P., 2001, *Modeling and Simulation of Mineral Processing Systems*, Amsterdam: Elsevier.

KOLAHI, S., JAHANI CHEGENI, M., 2020, *Investigation of Effect of Number of Lifters on Performance of Pilot-Scale SAG Mills Using Discrete Element Method.* Journal of Mining and Environment (JME), 11, 675-693.

KWAN, C. C., MIO, H., PAPADOPOULOS, D. G., CHEN, Y. Q., DING, Y. L., SAITO, F., A. BENTHAM, C., GHADIRI, M., 2005, *Analysis of the milling rate of pharmaceutical powders using the Distinct Element Method (DEM).* Chemical Engineering Science, 60, 1441 – 1448.

LAMECK, N. S., KIANGI, K. K., MOYS, M. H., 2006, *Effects of grinding media shapes on load behavior and mill power in a dry ball mill.* Minerals Engineering, 19, 1357–1361.

LAMECK, S. N., 2005, e*ffects of grinding media shapes on ball mill performance.* Master thesis, Faculty of Engineering and the Built Environment, University of the Witwatersrand.

LATCHIREDDI, S., MORRELL, S., 2003, *Slurry flow in mills: grate-pulp lifter discharge systems (Part 2).* Minerals Engineering, 16, 635-642.

LATCHIREDDI, S., MORRELL, S., 2006, *Slurry flow in mills with TCPL- An efficient pulp lifter for Ag/Sag mills*. Int. J. Miner. Process, 79, 174 – 187.

LATCHIREDDI, S.R., 2002, *modeling the performance of grates and pulp lifters in autogenous and Semiautogenous mills.* PhD thesis, JKMRC, University of Queensland.

LVOV, V., CHITALOV, L., 2021, *Semi-Autogenous Wet Grinding Modeling with CFD-DEM*. Minerals, 11, 1-17.

MAGDALINOVIC, N., TRUMIC, M., TRUMIC, M., ANDRIC, L., 2012, *The optimal ball diameter in a mill*. Physicochemical Problems of Mineral Processing, 48, 329–339.

MALEKI MOGHADDAM , M., RAHMANI DEHNAVI, S., HESAMI, R., BANISI, S., 2018, *An Investigation of charge shape and mill speed on power draw in tumbling mills.* Iranian Journal of Mining Engineering, 13,82-94.

MARINO-SALGUERO, J., JORGE, J., MENENDEZ-AGUADO, J.M., ALVAREZ-RODRIGUEZ, B., DE FELIPE, J.J., 2017, *Heat generation model in the ball-milling process of a tantalum ore*. Minerals & Metallurgical Processing, 34, 10-19.

MARYUTA, A. *Frictional Oscillations in Mechanical Systems*; Nedra: Moscow, Russia, 1993; p. 240.

MAVKO, G., MUKERJI, T., DVORKIN, J., AL IBRAHIM, M., 2018, *The Influence of Convex Particles' Irregular Shape and Varying Size on Porosity, Permeability, Elastic Bulk Modulus of Granular Porous Media: Insights: From Numerical Simulations.* Journal of Geophysical Research: Solid Earth, 120, 10563-10582.

MAYANK, K., MALAHE, M., GOVENDER, I., MANGADODDY, N., 2015, *Coupled DEM-CFD Model to Predict the Tumbling Mill Dynamics*, Procedia IUTAM, 15, 139-149.

MISHRA, B. K., RAJAMANI, R. K., 1991, t*he discrete element method for the simulation of ball mills.* Applied mathematical modeling, 16, 598-604.

MISHRA, B. K., RAJAMANI, R. K., 2001, *Three-Dimensional Simulation of Plant Size SAG Mills. International Conference on Autogenous and Semiautogenous Grinding Technology*, SAG 2001, 48 -57.

MISHRA, B.K., 2003, *review of computer simulation of tumbling mills by the discrete element method: Part I – contact mechanics.* Int. J. Miner. Process, 71, 73 – 93.

MISRA, A., CHEUNG, J., 1999, P*article motion and energy distribution in tumbling ball mills.* Powder Technology, 105, 222–227.

MOLYCOP, 2021, https://molycop.com.

MORRELL, S., 1993, *the prediction of power draw in wet tumbling mills.* PhD thesis, Department of Mining and Metallurgical Engineering, University of Queensland.

MORRELL, S., 2009, P*redicting the overall specific energy requirement of crushing, high pressure grinding roll and tumbling mill circuits.* Minerals Engineering, 22, 544-549.

MORRELL, S., 2016, *Modeling the influence on power draw of the slurry phase in Autogenous (AG), Semi-autogenous (SAG) and ball mills.* Minerals Engineering, 89, 148- 156.

MORRELL, S., 2019, *SME Mineral Processing & Extractive Metallurgy Handbook*, Englewood: Society for Mining, Metallurgy & Exploration.

MOYS, M. H., 1993, *A model of mill power as affected by mill speed, load volume, liner design.* The Southern African Institute of Mining and Metallurgy, 93,135-141.

NIETRO, L., AHRENS, M., 2007, *Gearless Mill Drive Protection Improvements and Its Behavior at Minera Escondida Ltda*. 2007 IEEE Industry Applications Annual Meeting, New Orleans, LA, USA, 23-27.

Outotec. Grinding Optimizer. Available online : https://www.mogroup.com/globalassets/saleshub/documents---episerver/grinding-optimizer-leaflet-web.pdf (accessed on 10 December 2020).

PANJIPOUR, R., BARANI, K., 2018, *the effect of ball size distribution on power draw, charge motion and breakage mechanism of tumbling ball mill by discrete element method (DEM) simulation.*" Physicochemical Problems of Mineral Processing, 54, 258-269.

PENG, Y., BAO, J., WANG, Z., 2016, *A Comparison of Two-Dimensional and Three-Dimensional Micromechanical Discrete Element Modeling of the Splitting Tests for Asphalt Mixtures.* ICTIM 2016, 28-37.

POWEL, M., VALERY, W., 2006, S*lurry pooling and transport issues in SAG mills.* SAG 2006, Vancouver, Canada, 133-152.

R. MORRISON, R., CLEARY, P. W., VALERY, W., 2001, *Comparing power and performance trends from DEM and JK modelling.* SAG2001, Vancouver, Canada, 284-300.

RAJAMANI, R. K., ALKAC, D., DELGADILLO, J. A., KUMAR, P. PAGE, D., FILLION, M., PELLETIER, S., 2011, *Pulp-lifter flow modeling study in a pilot scale mill and application to plant scale mills.* SAG2011.

RAJAMANI, R. K., KUMAR, P., GOVENDR, N., 2019, *The evaluation of grinding mill power models.* Mining, Metallurgy and Exploration, 36, 151-157.

RAZANI, M., MASOUMI, A., REZAEIZADEH, M., NOAPARAST, M., 2018, *Evaluating the Effect of Feed Particles Size and Their Hardness on the Particle Size Distribution of Semi-Autogenous (SAG) Mill's Product.* Particulate Science and Technology, 36, 867-872.

ROSE, H. E., EVANS D. E., 1956, *The dynamics of the ball mill, part I: Power requirements based on the ball and shell system.* Proc. Inst. Mech. Engineers, 773 - 783.

ROSE, H. E., EVANS D. E., 1956, *The dynamics of the ball mill, part II: the influence of the powder charge on power requirements.* Proc. Inst. Mech. Engineers, 784 – 792.

ROYSTON, D., 2000, *Curved pulp lifters for AG and SAG mills - current experience.* Proceedings of the SME Annual Meeting, Salt Lake City, Utah, 1-3.

ROYSTON, D 2005, *SAG mill pulp lifter design, discharge and backflow*, Proceedings of the SME Annual Meeting, Society of Mining Engineers, Salt Lake City, Utah, 1-6.

SHAHBAZI, B., JAFARI, M., PARIAN, M., ROSENKRANZ, J., S. CHEHREH CHELGANI, 2020, *Study on the impacts of media shapes on the performance of tumbling mills – A review.* Minerals Engineering, 157, 1-10.

SILVA, M., CASALI, A., 2015, *Modeling SAG milling power and specific energy consumption including the feed percentage of intermediate size particles.* Minerals engineering, 70, 156-161.

SIMBA, K. P., 2010, *effects of mixture of grinding media of different shapes on milling kinetics.* Master thesis, Faculty of Engineering and the Built Environment, University of the Witwatersrand.

SINNOTT, D., CLEARY, P.W., MORRISON, R.D., 2017, *Combined DEM and SPH simulation of overflow ball mill discharge and trommel flow*, Minerals Engineering, 108, 93-108.

SOLEYMANI, M.M., FOOLADI MAHANI, M., REZAEIZADEH, 2016, *Experimental observations of mill operation parameters on kinematic of the tumbling mill contents,* Mechanics & Industry, 408, 1-8.

SOLEYMANI, M.M., FOOLADI MAHANI, M., REZAEIZADEH, M., *2015, Experimental study the impact forces of tumbling mills.* Journal of process mechanical engineering, 231, 283-293.

SOLUTIONS, EDEM 2.6 User Guide, 2011.

TAVARES, L., 2017, A *Review of Advanced Ball Mill Modeling*. Powder and particle, 34, 106-124.

TAVARES, L.,RÉ, F. P., POTAPOV, A., MALISKA, C., 2020, *Adapting a breakage model to discrete elements using polyhedral particles*. Powder Technology, 362, 208-220.

TSAKALAKIS, K. G., STAMBOLTZIS, G. A., 2004, *Modeling the Specific Grinding Energy and Ball-Mill Scale-up.* IFAC Proceedings, 37, 53-58.

U.S. DOE, *Mining industry energy bandwidth study*, Washington, United States: U.S. Department of Energy, 2007.

VALERY. W., JANKOVIC, A., 2002, *The future of Comminution.* In: 34th IOC on mining and Metallurgy, Bor Lake, Yugoslavia, 287-298.

VAN NIEROP, M.A., GLOVER, G., HINDE, A.L., MOYS, M.H., 2001, *A Discrete element method investigation of the charge motion and power draw of an experimental two-dimensional mill*, Int. J. Miner. Process, 61, 77–92.

VENUGOPAL, R., RAJAMANI, R. K., 2001, *3D simulation of charge motion in tumbling mills by the discrete element method." Powder Technology*. 115, 157–166.

WALKER, J., HALLIDAY, D., RESNICK, R., 2011, *Fundamentals of Physics, Hoboken: John Wiley & Sons*.

WANG, M. H., YANG, R. Y., YU, A.B., 2012, *DEM investigation of energy distribution and particle breakage in tumbling ball mills.* Powder Technology, 223, 83–9.

WANG, X., YI, J., ZHOU, Z., YANG, C, 2020, *Optimal Speed Control for a Semi-Autogenous Mill Based on Discrete Element Method.* Processes, 8, 1-17.

WEERASEKARA, N. S., LIU, L.X., POWELL, M.S., 2016, *Estimating energy in grinding using DEM modeling." Minerals Engineering*, 85, 23–33.

WEERASEKARA, N. S., POWELL, M. S., CLEARY, P.W., TAVARES, L. M., EVERTSSON, M., 2013, *The contribution of DEM to the science of comminution.* Powder Technology, 248, 2-24.

WEERASEKARA, N.S., POWELL, M.S., 2014, *Performance characterisation of AG/SAG mill pulp lifters using CFD techniques*. Minerals Engineering, 63, 118-124.

YANG, W. C., 2003, *Handbook of Fluidization and Fluid−Particle System*, Marcel Dekker, New York.

YIN, Z., LI, T., PENG, Y., WU, B., 2018, *Effect of lifter shapes on the mill power in a ball mill.* IMMAEE 2018.

YIN, Z., PENG, Y., ZHU, Z., YU, Z., LI, T., 2017, *Impact load behavior between different charge and lifter in a laboratory-scale mill.* Materials, 10, 1-17.

ZHANG, J., BAI, Y., DONG, H., WU, Q., YE. X., 2014, *Influence of ball size distribution on grinding effect in horizontal planetary ball mill.* Advanced Powder Technology, 25, 983–90.

ZHU, Z. H., YIN, J. H., OUYANG, C. J., TAN, D. Y., QIN J. Q., 2019, *Modeling a Flexible Ring Net with the Discrete Element Method.* Journal of Engineering Mechanics, 146,1-12.